Computer Modeling in Engineering & Sciences

Tech Science Press

DOI: 10.32604/cmes.2022.020831

REVIEW

A Comparison of Shale Gas Fracturing Based on Deep and Shallow Shale Reservoirs in the United States and China

Qixing Zhang[1,2], Bing Hou[1,2,*], Huiwen Pang[1,2], Shan Liu[1,2] and Yue Zeng[1,2]

[1]State Key Laboratory of Petroleum Resources and Prospecting, China University of Petroleum (Beijing), Beijing, 102249, China

[2]Key Laboratory of Petroleum Engineering, Ministry of Education, China University of Petroleum (Beijing), Beijing, 102249, China

*Corresponding Author: Bing Hou. Email: binghou@vip.163.com

Received: 15 December 2021 Accepted: 27 March 2022

ABSTRACT

China began to build its national shale gas demonstration area in 2012. The central exploration, drilling, and development technologies for medium and shallow marine shale reservoirs with less than 3,500 m of buried depth in Changning-Weiyuan, Zhaotong, and other regions had matured. In this study, we macroscopically investigated the development history of shale gas in the United States and China and compared the physical and mechanical conditions of deep and shallow reservoirs. The comparative results revealed that the main reasons for the order-of-magnitude difference between China's annual shale gas output and the United States could be attributed to three aspects: reservoir buried depth, reservoir physical and mechanical properties, and engineering technology level. The current engineering technology level of China could not meet the requirements of increasing production and reducing costs for deep shale gas reservoirs; they had reached the beneficial threshold development stage and lacked the capacity for large-scale commercial production. We identified several physical and mechanical reasons for this threshold development stage. Deep shale reservoirs were affected by the bedding fracture, low brittleness index, low clay mineral content, and significant areal differences, as well as by the transformation from elasticity to plasticity, difficulty in sanding, and high mechanical and strength parameters. Simultaneously, they were accompanied by six high values of formation temperature, horizontal principal stress difference, pore pressure, fracture pressure, extension pressure, and closure pressure. The key to deep shale gas horizontal well fracturing was to improve the complexity of the hydraulic fracture network, form adequate proppant support of fracture surface, and increase the practical stimulated reservoir volume (SRV), which accompanied visual hydraulic discrete network monitoring. On this basis, we proposed several ideas to improve China's deep shale gas development involving advanced technology systems, developing tools, and supporting technologies in shale gas exploration and development in the United States. These ideas primarily involved stimulation technologies, such as vertically integrated dessert identification and optimization, horizontal well multistage/multicluster fracturing, staged tools development for horizontal wells, fractures network morphology monitoring by microseismic and distributed optical fiber, shale hydration expansion, soak well, and fracturing fluid flow back. China initially developed the critical technology of horizontal well large-scale and high-strength volume fracturing with a core of "staged fracturing with dense cutting + shorter cluster spacing + fracture reorientation by pitching + forced-sand addition + increasing diameter perforating + proppant combination by high strength and small particle size particles". We concluded that China should continue to conduct critical research on theories and technical methods of horizontal well fracturing, suitable for domestic deep and ultra-deep marine and marine-continental sedimentary shale, to support and promote the efficient development of shale gas in China in the future. It is essential to balance the relationship between the overall utilization degree of the gas reservoir and associated economic benefits and to localize some

essential tools and supporting technologies. These findings can contribute to the flourishing developments of China's deep shale gas.

KEYWORDS

Deep and shallow shale in the United States and China; physical and mechanical properties; multistage/multicluster; fractures network monitoring; soak well and flow back

1 Introduction

According to National Bureau of Statistics of China and the *Energy Development Report of China 2020*, China's cumulative natural gas production in 2019 was 175.362 billion m^3. The output of unconventional natural gas, such as tight gas, shale gas, and coalbed methane, accounted for more than 30% of this, increasing 23% over the past year. In the same year, China's newly proved gas reserves reached 1.4 trillion m^3, which was an increase of 68.0% over the previous year. Nevertheless, China's gas resource external dependence reached 43.7%, and the import volume was 134.605 billion m^3 (a year-on-year increase of 6.9%). According to the *China Mineral Resources 2019* report, China is rich in shale gas resources, and the geological resources of shale gas with a depth of 4,500 m reached 122 trillion m^3, less than 4.79% is ascertained.

The particle size of shale in China usually is less than 3.9 μm. The shale reservoir is composed of dark and black pure shale that is rich in clay minerals or siliceous minerals and organic shale, argillaceous carbonate rock, and siltstone [1–3]. The mineral composition of shale generally includes 30%–50% clay minerals, 15%–25% quartz, and 1%–20% organic matter. This shale gas came from biological or thermal maturation, and the shale gas is authigenic and autochthonous; in other words, shale is both a gas source rock and a reservoir stratum. The shale gas can be categorized as free gas and adsorbed gas, and shale gas can flow, slip, and diffuse in the matrix and then fracture [4–6]. The content of adsorbed gas varies from 20% to 85% with changes in reservoir pore pressure and temperature [7,8].

The exploration and development of deep and shallow shale gas at home and abroad has involved horizontal or vertical well drilling, horizontal well multistage fracturing, shale gas production, gas storage, and gas transportation (Fig. 1).

The stimulation and effective development of shale gas has faced the following three vital mechanical problems:

1. Characterization of shale mechanical behavior: The shale macroscopically has developed faults, joints, and tectonic interleaving structures. Mesoscopically, the shale has had pores, microfractures, and weak surfaces. These properties have made the shale reservoirs present discontinuous, inhomogeneous, and anisotropic traits. Consequently, it has been complicated to quantify the physical parameters, characterize the mechanical behaviors, and establish a constitutive model for shale reservoirs. Meanwhile, significant confusion has surrounded the transformation from elasticity to plasticity, variations in porosity and permeability, damage and fracture of shale reservoir, and multifield coupling analysis under deeper reservoir conditions [9].

2. Shale gas macro- and microtransport mechanism: The shale pore structure can be categorized into the matrix, microfracture, and natural fracture. The porosity and permeability of the matrix has been extremely low, and adsorbed gas and free gas often were enriched in the microfractures. The porosity and permeability of microfractures can be used to determine the degree of enrichment for shale gas. Horizontal well multistage fracturing is essential for commercial and efficient exploitations and to create hydraulic fracture flow channels. Shale gas production involves multiscale flow from the micro-nano to the millimeter, adsorption and desorption between adsorbed gas and free gas, multiphase flow under complex fractures network, and fluid mechanics of downhole strings [10–13].
3. Multistage fracturing stimulation of shale reservoir: Multistage/multicluster fracturing has been the leading technology for reservoir stimulation, which could be used to effectively communicate the micro- and natural fractures enriched in the shale gas and to form a complex fracture network. Multistage/multicluster fracturing stimulation is related to several construction technologies, such as vertically integrated dessert identification and optimization, staged tools development, stage and cluster spacing setting, fractures network morphology monitoring, high-strength sanding, fracturing fluid optimization, shale hydration expansion, soak well, and fracturing fluid flow back. Previous scholars have utilized numerical simulation methods to characterize the shale gas transport and fracture propagation, such as the finite difference method, discrete element method, finite element method, extended finite element method, and molecular dynamics [14–16].

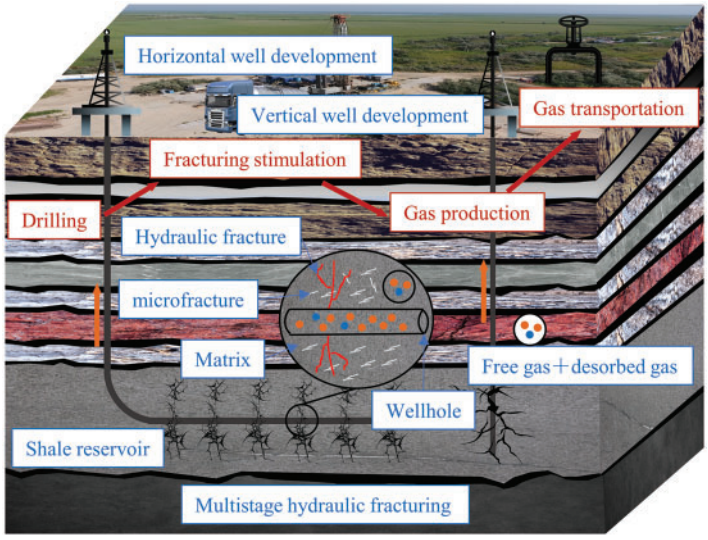

Figure 1: Basic flow of shale gas exploitation

The *Shale Gas Development Programming during the Chinese National 13th Five-Year Plan (2016–2020) Plan* noted that China's goal by 2030 was to make breakthroughs in the development of marine facies, continental facies, and marine-continental transitional facies shale reservoirs. The plans included discovering a series of significant new shale gas fields, realizing the scale and effective development, and achieving shale gas production of 80–100 billion m^3 by 2030. The United States, Canada, and China have successively recognized large-scale commercial exploitation of shale oil and gas [17,18]. According to the statistical data of the China National Petroleum Corporation (CNPC)

in 2021, the top five countries with technically recoverable shale gas resources accounted for half of the total known resources in the world. Among them, China ranked first, with 31.58×10^{12} m^3 of the technically recoverable resources, accounting for 14.72% of the world's total. Argentina and Algeria followed, with technically recoverable resources of 22.70×10^{12} m^3 and 2.02×10^{12} m^3, respectively. The United States ranked fourth with 17.63×10^{12} m^3 and Canada ranked fifth with 16.22×10^{12} m^3 of the technically recoverable resources. In contrast, Russia, which has the most proven gas reserves globally (according to the *2022 Annual Report* of BP p.l.c.), vigorously developed shale oil from 2015 to 2025. According to the U.S. Department of Energy, Russia has the world's most technically exploitable shale oil resources, followed by the United States, with China ranking third. Only the United States and Canada have been able to exploit shale oil resources with commercial quality. The United States has been a pioneer in the success of the shale gas revolution and achieved energy self-sufficiency for the first time in 2018. Many experiences and technologies of other countries and regions are worth learning from.

China implemented the first shale gas well fracturing in 2010, which was fully learned from the development and stimulation models in North America. Based on the national geomechanical characteristics, China has created a theoretical and technical system suitable for fracturing stimulation of medium and shallow marine shale. This study first compared the shale gas exploration and development process and the cumulative production between the United States and China. The breakthrough in horizontal well multistage fracturing is the key technology attributed to the success of the shale gas revolution. Since comparing the physical and mechanical geological reservoir conditions in the United States and China, it was found that reservoir buried depth was the main factor that caused the production gap except for the disparities in development technology. The geological conditions of shale gas in China were less conventional and primarily reflected an older geologic age under a deeper burial depth, lower resource abundance, and uneven distribution of shale gas. Finally, combined with the reality of shallow shale gas development in China and the successful experience of the U.S. shale gas revolution, this study explored five critical problems identified in horizontal well multistage/multicluster fracturing stimulation. Finally, we proposed suggestions to accelerate the exploration of shale gas in China.

2 Evolution of Shale Gas Fracturing between the United States and China

Most of the previous literature only focused on one aspect of the shale gas development process. We mainly compare government support and technological development from the time axis on the development history. The key to the success of the American shale gas revolution can be found in its development of horizontal well and fracturing stimulation technologies, national support in policy, and exploration of more commercial oil and gas fields. The evolution of shale gas for the United States is illustrated in Fig. 2. In 1812, Hart company first produced shale gas at 21 m depth in Fredonia, New York, with meager output. Mitchell Energy applied drag-reducing water to the fracturing stimulation of the Barnett shale gas field with pronounced effect, and the first industrial shale gas flow appeared [19]. The United States employed vertical well fracturing from 1997 to 2002, but the stimulation effect was not significant. Devon energy carried out horizontal well multistage fracturing tests in the Barnett shale gas field in 2002, and shale gas production began to increase more rapidly (Fig. 3). Since then, the United States has expanded horizontal well slick-water fracturing, horizontal well multistage/multicluster fracturing, CO_2 fracturing [20,21], N_2 fracturing [22,23], liquid petroleum gas–based fracturing [24], explosive fracturing, repeated fracturing, simultaneous fracturing, zipper fracturing, and "well factory" fracturing (proposed by EnCana) [25–29].

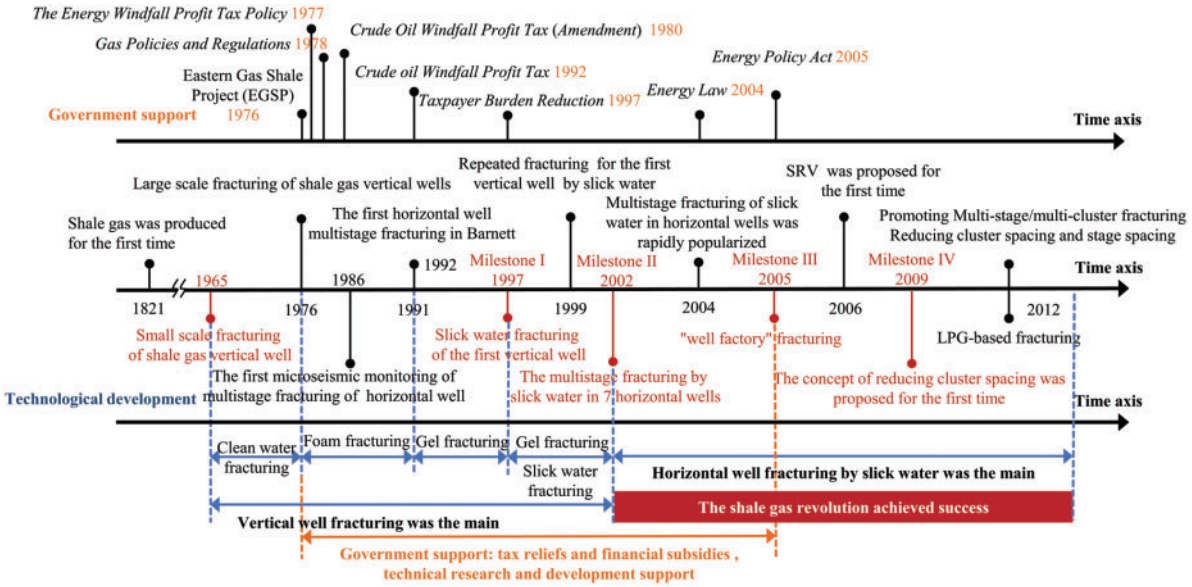

Figure 2: Evolution of shale gas in the United States

The U.S. government has issued many policies and granted financial support to assist the development of shale gas. The U.S. government launched the Eastern Gas Shale Project (1976–1992) to evaluate the geological reserves of domestic shale gas under the oil crisis. The United States promulgated several policies for financial subsidies and tax reliefs, including the Energy Windfall Profit Tax Policy 1977, Gas Policies and Regulations 1978, Crude Oil Windfall Profit Tax 1992, and Taxpayer Burden Reduction 1997. Energy Law 2004 stipulated that the government needed to provide US$45 million a year for unconventional development, such as shale gas [30–35]. The Energy Policy Act 2005 promulgated regulation specifying that a particular subsidy should be given to unconventional oil and gas wells. In addition, the United States set up plenty of unconventional oil and gas research funds for universities or research institutions to carry out basic theoretical and exploration technology research (Fig. 2).

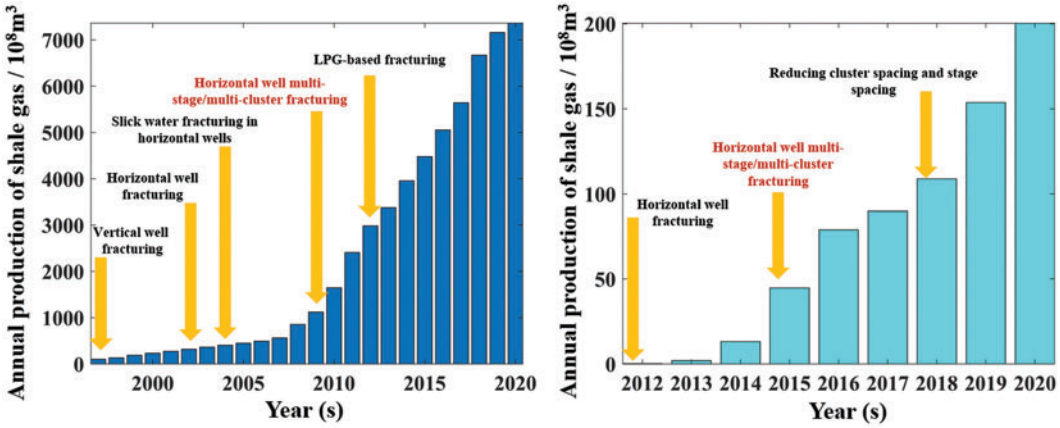

Figure 3: Comparison of annual shale gas production between the United States and China (modified from Zhao et al. [36])

The annual production of the Barnett shale gas field in 2003 was 7.5 billion m^3, accounting for 28% of the output of the whole country. The United States subsequently successfully developed industrial shale gas fields, such as Haynesville, Marcellus, Fayetteville, Utica, Woodford, Antrim, and New Albany, as well as tight oil fields, such as Bakken, Eagle Ford, and Permian. The cumulative fracturing of shale gas wells in the United States exceeded 100,000 shale gas wells, and the output was 736.2 billion m^3, which was currently the largest shale gas produce country globally. The average recoverable gas of a single shale well in the United States was 5000–10200 m^3. In comparison, the average recoverable gas of a single well in China was 3000–37000 m^3. The order-of-magnitude difference for the annual output of shale gas between the United States and China is shown in Fig. 3.

The shale gas industry developed relatively late in China, but its development rate was fast (Fig. 4). The National Natural Science Foundation of China awarded Jinchuan Zhang, China University of Geosciences, the first shale gas special project in 2002. Jinchuan Zhang reported shale gas in China's HowNet database for the first time in 2003. China's Ministry of Land and Resources began to conduct geological screening for shale gas in China, and in 2007, CNPC and Newfield Exploration, a U.S. company, jointly developed shale gas in the Weiyuan region for the first time. In 2008, CNPC drilled the Changxin 1 well for geological evaluation in the Changning region. This well confirmed that the underground reservoir was rich in shale gas, which signaled a substantive stage for China's shale gas development. CNPC and China Petroleum & Chemical Corporation (Sinopec) first implemented shale gas vertical well fracturing well Wei 201 and well Fangshen 1, respectively, in 2010, and horizontal well fracturing in well 201-H1 and well Jianye HF-1, respectively, in 2011. The fracturing design, fracturing tools, and fracturing fluid of all of the wells were provided by Schlumberger, Baker Hughes, and BJ Services Co. (BJS). From 2012 to 2013, CNPC and Sinopec used domestic slick water for the first time in the fracturing construction of well Wei 204 and well Yuanye 1, which marked the beginning of localization of shale gas fracturing fluid in China. CNPC launched China's first microseismic monitoring system, and Sinopec developed a type 3000 fracturing truck in the same year. CNPC researched and developed the first set of a domestic soluble bridge plug in 2016. CNPC and Sinopec installed repeated fracturing in Changning H3-6 well and Jiaoye 9-2Hf well, respectively, in 2017, which demonstrated that shale gas domestic comprehensive technologies for exploration and development were moving toward localization. In 2020, Sinopec successfully implemented fracturing stimulation in Pushun 1 well with a vertical depth of 5969 m in Liangping District, which was the deepest well depth before 2020.

The Chinese government also provided a series of financial subsidies, tax relief, and technical support for shale gas development. The United States and China signed the "Memorandum of Understanding on Cooperation in the Field of Shale Gas" in 2009. China signed the "China–United States Work Plan of Shale Gas Resources Working Group" in 2010 and established the China National Energy Shale Gas R&D (Experiment) Center. The aim was to promote the joint development of oil and gas resource assessment, equipment research and development, and policy exchanges between the United States and China. China's state council approved the *Outline of Prospecting Breakthrough Strategic (2011–2020)* in 2011 and listed shale gas as the 172nd independent mineral species. The *Government Work Report 2012* noted that fracturing stimulation was the core and critical technology for shale gas exploration and effective development. *Shale Gas Industry Policy 2013* encouraged friendly cooperation at home and abroad. The *Notice on Introducing Subsidy Policies for Shale Gas Development and Utilization 2012* stipulated the administrative subsidy policies for shale gas development from 2012 to 2020 and then extended the subsidy period to 2023. The *Notice on Tax Policy Issues Related to the in-depth Implementation of the Western Development Strategy 2011* and

the *Notice on Reducing Resource Tax for Shale Gas 2018* stipulated that taxes should be reduced for domestic and foreign oil and gas enterprises.

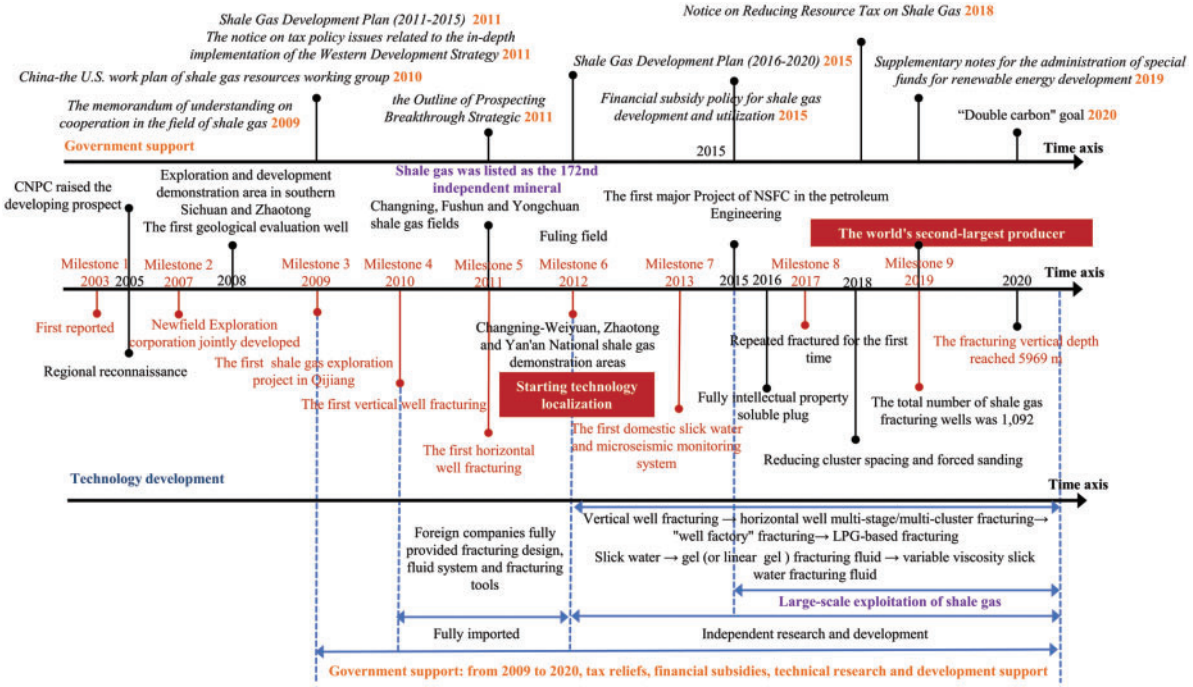

Figure 4: Evolution of shale gas in China

According to the Ministry of Land and Resources evaluation results in 2015, China's technically recoverable shale gas resources were 21.8 trillion m^3, including 13.0 trillion m^3 of marine facies, 5.1 trillion m^3 of marine-continental transitional facies, and 3.7 trillion m^3 of continental facies. China identified 44 shale gas exploration areas covering an area of 144,000 km^2. Shale gas demonstration areas were distributed primarily in Sichuan, Yunnan, and Chongqing. To date, five national shale gas demonstration zones have been established: Changning-Weiyuan (2012, CNPC), Zhaotong (2012, CNPC), Yan'an (2012, CNPC), Fuling (2013, Sinopec), and Fushun-Yongchuan (2016, CNPC). The total number of shale gas fracturing wells in China had reached 1092 by 2019. China had become the second-largest shale gas producer globally, continuously developing new fracturing technology and expanding production.

3 Comparison of Geological and Development Characteristics of Deep and Shallow Shale

The *Geological and Mineral Industry Standards of the People's Republic of China (DZT0254-2014)* defined the buried depth of shale formation at 3500–4500 m as a deep reservoir, and that exceeding 4500 m as an ultra-deep reservoir [37–39]. Currently, the central exploration, drilling, and development technologies for medium and shallow marine shale strata with a buried depth of less than 3500 m in Changning-Weiyuan, Zhaotong, and other regions tends to be mature. Deep shale reservoirs also are rich in organic shale gas, but the existing horizontal well development technologies for medium and shallow formations have been insufficient. The deep shale gas has reached the beneficial threshold of development but lacks the capacity of large-scale commercial production. Therefore, it is essential to

explore the differences between deep and shallow shale and support the commercial exploitation of deep shale gas.

The most significant difference between shallow, deep, and ultra-deep shale reservoirs is the in situ stress magnitude. With an increase in buried depth, the confining pressure borne by the shale reservoir gradually increases, which results in increments of rock strength and transformation from brittleness to plasticity. Furthermore, shale reservoirs possesses more remarkable plasticity before rock failure and lower brittleness index as the confining pressure increases. Consequently, the first construction technique to be adjusted was to break the modes of vertical well or horizontal well drilling. This work required a combination of different rock-breaking tools (e.g., bit types with other structures), breaking patterns (e.g., impacting, crushing, shearing, cutting, and grinding), and breaking mechanical parameters (e.g., weight on bit (WOB), speed of revolution, and hydraulic parameters) [40–42].

The pore and fracture structures were compressed as the degree of rock compaction increased, and the porosities and permeabilities showed a downward trend. These changes resulted in a drastic increase in the difficulty of oil and gas flow. Wang et al. [43] used a scanning electron microscope (SEM) to conduct a slice analysis of black shale at different depths of the Longmaxi Formation. The 3168 m shallow black shale was relatively developed and had more inorganic pores (red dots in Fig. 5), whereas the 3615 m deep shale had more organic pores and microfractures (green dots), and the face rate of the former was higher (Fig. 5). In addition, more bedding fractures were developed in the deep shale, which enabled the fracturing stimulation to form a complex fracture network.

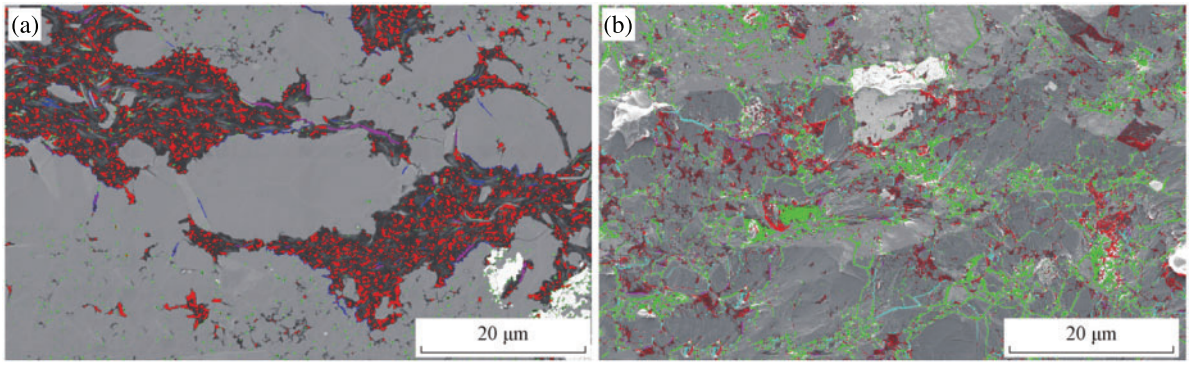

Figure 5: Micropore structure of shale at 3168 m and 3615 m buried depth

The characteristics of deep shale reservoirs include the development of bedding fracture, low brittleness index, low clay mineral content and significant areal differences, transformation from elasticity to plasticity, difficulty in sanding, and high mechanical and strength parameters. Moreover, these reservoirs are accompanied by six high values of formation temperature, horizontal principal stress difference, pore pressure, fracture pressure, extension pressure, and closure pressure [44–46]. Under the functions of sedimentation and diagenesis, the "fragment" characteristics of deep shale have been strengthened, and shale reservoirs have developed fully filled natural fractures. The stratigraphic sequence of deep shale has been increased, and the structural and fault movements of the overlying strata and target stratum reservoir became more complex. The pressure coefficient of the deep shale reservoir was more significant, and often was accompanied by abnormally high pressure. The pore structures of deep shale reservoirs were changeable and developed microfractures with long pore evolution time continued. The adsorption capacity of deep shale reservoirs decreased under high temperature and high pressure, which led to the total gas content and the proportion of free gas

increasing [47,48]. The deep shale reservoir's fracture pressure and extension pressure have been high because of the tremendous differences in horizontal principal stress. The deformation space and hydraulic fracture width were small, which created low conductivity for shale gas. It was difficult to change the direction of hydraulic fractures of deep shale formation, which resulted in simple spatial forms of hydraulic fractures. Thus, it was challenging to communicate multilayer bedding surfaces for hydraulic fractures [49–53]. The interference among horizontal multifractures for deep shale reservoir increased further, which created significant challenges for sand, adding scale and strength.

Consequently, it has been difficult to set reasonable segment spacing and cluster spacing and laborious to enlarge the stimulated reservoir volume [54,55]. The comparisons of physical properties for deep and shallow shale reservoirs are summarized in Table 1. The noted factors have led to low initial gas production and a rapid decline rate when the shale gas well began to exploit after fracturing stimulation.

Table 1: Comparison of physical property conditions for deep and shallow shale reservoirs

	Type	Medium shallow shale reservoir	Deep shale reservoir
Material composition	Clay minerals	Higher	Lower and regional inequality
	Fracture/fault	Natural fractures developed, faults underdeveloped, with weak stress sensitivity	Microfractures/bedding/fault developed (closing and filling), with strong stress sensitivity
Structural features	Pore structure	Lower compaction degree	Higher compaction degree, low face rate, high rock density
	Strength parameters	Lower	Higher
	Temperature	Lower (90°C–120°C)	Higher (120°C–150°C)
	Physical parameters	Relatively better	Relatively worse, strong heterogeneity
	In situ stress	Lower overburden pressure	Higher (overburden pressure, horizontal principal stress difference), difficult to form complex fracture networks
Physical and mechanical characteristics	Brittleness index	Higher	Lower fracture, breaking, and fracturing were more difficult

(Continued)

Table 1 (continued)

	Type	Medium shallow shale reservoir	Deep shale reservoir
	Fracturing pressure	Lower	Higher, lower fracture width, more incredible sanding difficulty, poor conductivity
	Propagation pressure	Lower	Higher, fractures were not easy to turn
	Pore pressure coefficient	Lower (1.2–2.0), a tremendous difference	Higher (1.8–2.2), a smaller difference
	Closing pressure	Lower (45–70 MPa)	Higher (90–100 MPa)

We identified two difficulties in deep shale reservoir fracturing stimulation. First, the early trial productions of deep shale reservoirs were low, although they showed excellent development potential, whereas the required threshold production for drilling and fracturing was high. Then, we noted essential differences between the middle-shallow and deep shale formation of fracture network stimulation operations because of the previously noted in the six high values. In addition, the hydraulic fractures could not be effectively supported, and the proppant was easily embedded in the fracture surface in the later stage of production.

4 Comparison of Shale Reservoir Conditions in the United States and China

Marine facies dominated American shale and were widely distributed in the three major basins, including most organic-rich shale strata from the Paleozoic to the Mesozoic. The Barnett shale gas field is located in the Fort Worth Basin in North Central Texas, a foreland basin formed by the orogenic movement of the Ouachita Mountains. The Appalachian Basin in the Eastern United States has a Marcellus shale gas field, and a foreland basin formed by Acadian Mountain orogeny. The Haynesville shale gas field is in the North Louisiana Salt Basin located between Texas and Louisiana and is a craton basin with extensional tectonic function. The exploration and development of the Barnett shale field occurred the earliest, and Marcellus is currently the largest shale gas field in the United States.

China's recoverable shale gas resources total about 26 trillion m^3, which is roughly equivalent to the United States. Nevertheless, the physical property conditions of shale gas reservoirs in China are not as good as in the United States. Shale gas in China is distributed across extensive basins, such as Sichuan, Ordos, Bohai Bay, Songliao, Jianghan, Turpan Hami, Tarim, and Junggar. The Sichuan Basin was the earliest and the most productive basin in China.

4.1 Comparison of Reservoir Physical Characteristics

The geological reservoir conditions in China are more complex than those in the United States (e.g., tectonic evolution, sedimentary environment, and thermal evolution), and there are significant differences in the generation and enrichment of shale gas in different regions. The first difference for shale gas reservoirs between the United States and China is the buried depth. China's shale gas reservoirs mainly are deep strata (higher than 3500 m) with thin interbeds, while the United States is

dominated by middle-shallow formation (2500–3500 m). The three types of shale in China are marine, marine-continental, and continental sedimentary shale, and the marine facies are mainly sedimentary and unevenly distributed [56,57]. The United States primarily has marine shale, and the distribution is relatively homogeneous. According to the parameters of shale gas abundance, the organic carbon content, gas content, and thermal evolution degree R_o of China have been lower than those of the United States (Table 2). Furthermore, the structural transformation of shale reservoirs in China has been substantial, and the shale reservoirs had discontinuous features, such as multiscale fractures, joints, and cross lithology. Shale lithology was different from sandstone and carbonate rock.

Table 2: Comparison of physical properties of shale reservoirs between the United States and China

Features	Shale reservoirs in China	Shale reservoirs in the United States
Buried depth	Mainly > 3500 m, deep	Mainly 2500–3500 m, medium-shallow
Reservoir thickness	Mostly thin interbeds, lower reserve abundance	Larger thickness, extensively distributed, higher reserve abundance
Structure	Complex, multiple tectonic movements, developed faults	Single tectonic uplifting, few faults
sedimentary facies	Marine, marine-continental, and continental, marine dominated	Marine dominated, more homogeneous
Total organic carbon, TOC	Medium, mainly 1%–5%	Abundant, mainly 5%–10%
Gas content	Low (average 1–3 m^3/t)	High (average 3–6 m^3/t)
Thermal evolution, R_o	Obvious change, marine facies ($R_o > 2.0\%$), continental facies ($R_o < 1.3\%$)	Moderate change (R_o was 1.1%–2.0%)
Ground condition	Multiple mountains in the south, less water in the north, pipe network was generally underdeveloped	Plains or hills, high-quality water source, developed pipe network

We identified some differences in shale reservoirs' physical and mechanical parameters in different areas between the United States and China. In this study, we counted the physical and mechanical parameters of eight shale gas fields in Barnett, Marcellus, Haynesville, Woodford, Antrim, Eagle Ford, New Albany, and Fayetteville in the United States (Table 3). In China, the Sichuan Basin possessed the largest reserves of organic shale gas and the highest development potential (Table 4). Therefore, in this study, we analyzed the characteristics of the physical and mechanical parameters of different strata only in the Sichuan Basin. Furthermore, the physical and mechanical parameters were affected by confining pressure, temperature, bedding, loading direction, water saturation, and organic content, and these factors had to be fully considered [58–64].

Table 3: Summary of physical and mechanical parameters of shale in the United States

Fields	Barnett	Marcellus	Haynesville	Woodford	Antrim	Eagle ford	New albany
Region	Fortworth basin	Appalachian basin	Gulf of mexico	Anadarko basin	Michigan basin	Texas	Illinois basin
Basin type	Foreland	Foreland	Foreland	Foreland	Craton	-	-
H	1220–3990	1220–3990	1220–3990	1829–3353	183–730	1200–4500	152–1494
E	15–72	13–25	14–35	9.25–23.47	13–35	30.58	9–11
G	4.3–10.3	6.7–14.2	14.8–17.9	12.4–14.2	8.5–14.4	5.12–9.89	4.67–8.12
v	0.095–0.35	0.22	0.24	0.1–0.25	0.2–0.3	0.212–0.30	0.11–0.30
K	1.47–12.92	4.17–17.89	6.88–14.47	9.6–12.5	13.5	5.5–37	12.4–26.7
σ_c	160–220	46.9–143.2	50.7–184.3	43.50–124	36.89–146.77	116.2	20–110
c	12.97–37.7	23.7–36.9	19.6–29.7	12.51	18.9	5.7–14.3	20.2–36.3
θ	26.83–31.9	30.5–37.5	36.66	14	28.88	19.4–21.7	17.2
k	>2.0	0.13–0.77	<0.05	0.1–0.2	0.001–0.01	0.03–1.1	0.01–1.9
φ	4–5	10	4–12	3–9.0	9.0	5–8	1–7.0
ρ	2.295–2.5	2.34	2.46	2.56	2.66	2.6–2.71	2.38–2.42

Note: Buried depth, H, m; Young's modulus; E, GPa, shear modulus; G, GPa, Poisson's ratio; V, -, bulk modulus; K, GPa, compressive strength; σ_c, MPa, cohesion; c, MPa, internal friction angle, θ, °; permeability, k, mD; porosity, φ, %; density, ρ, g·cm^{-3}.

Table 4: Summary of physical and mechanical parameters of shale in Sichuan Basin

Fields	Longmaxi formation					Wufeng formation	Xujiahe formation
Region	Changning	Weiyuan	Fuling	Zhaotong	Pengshui	Middle-upper yangtze	Southern sichuan
Basin type	Craton	Craton	Craton	Foreland	Craton	Craton	Foreland
H	2501.5	2573–3513	2645	2030–2950	3000–4200	2312–2496	800–5900
E	20.5–31.4	29.25	20.26	35	25–50	6.3–38.6	11–51.85
G	18.3–21.2	12–16.1	14.8–17.9	9.2–17.3	12.5–19.8	12–16.1	17.28–29.33
v	0.18–0.24	0.19–0.3	0.174	0.2	0.101–0.318	0.19–0.247	0.19–0.30
K	8.8–12.4	9.7–14.6	7.6–13.7	11.7–25.3	9.823	11.2	14.71–33.54
σ_c	48–168	165–181	62–123	46–118.6	46.8–126.7	136.6	155–269
c	34.8	31.9–46.8	30.1–44.4	32.7–39.8	33.64–46.85	31.9–34.3	11.1–18.16

(Continued)

Table 4 (continued)

Fields	Longmaxi formation					Wufeng formation	Xujiahe formation
θ	30.7–38.6	26.8–33.5	26.4–33.2	30.4–39.7	28.63–32.7	28.63–32.7	21.67–47.3
k	0.029	0.04–0.77	0.215	0.07	0.36–0.77	0.21	0.11–0.69
φ	4.3	1.68–7.03	2.78–7.08	2.0–5.0	0.36–7.72	1.65–4.52	1–8.23
ρ	2.3–2.8	2.3–2.8	2.51–2.73	2.49–2.66	2.486–2.55	2.23	2.48–2.71

The micropore and fracture structure of shale caused a significant impact on the flow capacity, gas storage capacity, and mechanical properties, which revealed whether shale gas wells could achieve high production. The porosity and permeability of shale reservoirs were both low, porosity generally was 2%–15%, and permeability was less than 2 mD. The permeability varied significantly with the degree of fracture development [65]. Most of the shale pores were nanometer scale, divided into organic matter pores, intragranular corrosion pores, dissolved pores between grains, and microfractures. Among them, organic matter nanopores and intragranular corrosion pores were the most common. The International Union of Pure and Applied Chemistry classified the shale nanopores as micropores (pore diameter < 2 nm), mesopores (2–50 nm), and macropores (>50 nm). The pore size was classified as "multipeaks" and bimodal patterns. Micropores and mesopores accounted for the highest proportion in shale in terms of the pore volume. Micropores (especially nano micropores) were affected primarily by TOC; mesopores and macropores were dominated by clay minerals (particularly illite content) [66–68].

The porosity of commercially developed shale gas reservoirs generally had to exceed 4%, to align with the achievement of the shale gas revolution in the United States. The buried depth of shale gas reservoirs in the United States ranged from 1200 to 4500 m, most of which were medium and shallow strata. The shale porosity ranged from 1% to 12%, and matrix permeability changed from 0.001 to 2 mD. The porosity and permeability could increase if the reservoirs were in a fault zone or fracture development zone. In this case, the maximum porosity could reach 11%, and the fracture permeability was about 2 mD. Fields with high porosity in the United States included Haynesville (4%–12%), Marcellus (10%), Antrim (9%), Woodford (39%), and Eagle Ford (5%–8%), and these gas fields met the standards of commercial development.

The buried depth of shale in the Sichuan Basin was 800–5900 m, most of which was concentrated in the middle and deep strata. The highest porosity of shale in the Sichuan Basin was only 8% (Triassic Xujiahe formation), with an average of 1.65%–4.52%, and the permeability range was 0.029–0.77 mD. The porosity and permeability of U.S. shale were higher than those of Chinese shale. Moreover, the development degree of shale fractures had a meaningful influence on the physical and mechanical properties, including porosity, permeability, strength, and brittleness. The Antrim field (0.001–0.01 mD), Haynesville field (<0.05 mD), Changning region (0.029 mD), and Zhaotong region (0.029 mD) had relatively low permeabilities. The areas with relatively developed natural fractures generally possessed good permeability (>0.215 mD), such as Barnett field (which exceeded 2.0 mD).

4.2 Comparison of Reservoir Mechanical Properties

The Young's modulus of U.S. shale ranged from 9 to 72 GPa, and that of China's shale varied from 6 to 52 GPa (see Tables 3 and 4). The Young's modulus of shale increased with the buried depth, whereas the Poisson's ratio decreased with the buried deep, but the trends differed in different areas. The range of the Poisson's ratio of U.S. shale was 0.095–0.35, and that of China's shale was 0.101–0.35. We found little difference between the two countries, and the upper limit value of the Poisson's ratio was 0.35 for both. The brittleness of shale was closely related to the Young's modulus and Poisson's ratio: the higher the Young's modulus, the lower the Poisson's ratio and the higher the brittleness. High brittleness could form a complex fracture network and improve shale gas production and recovery degree. In the United States, Barnett shale had the highest compressive strength of 160–220 MPa, while in China, the Triassic Xujiahe formation in the Sichuan Basin had the highest compressive strength.

In comparison, the buried depth and compressive strength of shale in China were higher than in the United States. The deformation and failure of shale were affected by buried depth, confining pressure for testing, bedding, loading direction, temperature, and water saturation. Thus, compressive strength featured a wide range of variations. The number of generative microfractures before rock failure occurred could be reduced under high compressive strength, which was not conducive to fracturing stimulation measures [69]. Compressive strength was a symbolic parameter that could characterize rock deformation and failure. Rock fracture was obvious under low confining pressure, and splitting failure became the dominant mechanism, whereas shear failure was the primary mechanism under high confining pressure. The gradual enhancement of the deformation capacity under confining pressure resulted from the weak competition between rock grains boundary failure and rock grains plastic deformations [70,71].

We found many primary microfractures in shale. They could be compacted gradually or expanded into new fractures and then connected, converged, and expanded with other fractures until the shale was fully destroyed. The process of shale loading to the failure involved the compaction and expansion of primary fractures, the initiation and propagation of secondary fractures, and interconnections between multiple fractures. The elastic deformation was closely related to the mineral composition, mineral arrangement, and loading direction during loading [72,73]. employed an electron microscope to scan the microstructure of horizontal bedding shale samples before and after loading. They pointed out that there were many primary micropores and pore structures in the shale and found that microfractures often developed along the mineral boundary (Fig. 6). The lower shale contained many primary microfractures in the original state, which extended extensively along the bedding direction to form a microfracture group (weak bedding plane) (Fig. 6a). The original microfractures in the vertical loading direction were compacted and closed after imposed loads, and multiple microfractures were generated in the parallel loading direction (Fig. 6b). This featured a different crystal pore structure for various rocks with varying compositions of mineral. For example, the intergranular pores of carbonate minerals were larger. The grains were compacted and bent, and the minerals were extruded and deformed under the load action (Figs. 6c and 6d).

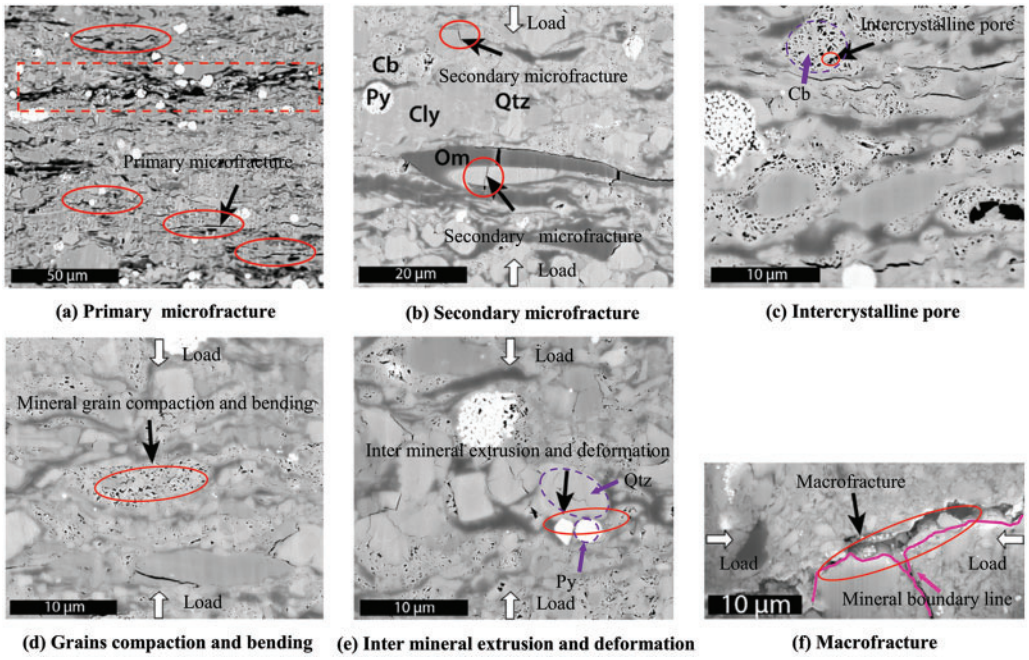

Figure 6: Microstructure changes of shale before and after loading

Note: Cb-mineral particle carbonate, Py-pyrite, Cly-clay, Qtz-quartz, Om-organic matter.

5 Key Fracturing Technology from U.S. Achievements

The deep shale reservoirs in Southwest China had fewer single-stage perforation clusters, small perforation diameters, low sand additions for single-stage fracturing, low sand ratios, and rugged fracturing construction. The fracturing operation parameters of the Jiaoye 1HF well in China imitated those of a well in Woodford fields, which were developed commercially (see Table 5). Unexpectedly, shale gas production of China after fracturing was only 5×10^4 m^3/d, and the reduction of the production rate in half a year exceeded 50%. Therefore, it was necessary to develop shale gas more efficiently in combination with China's geological and engineering conditions for shale reservoirs.

Table 5: Comparison of fracturing parameters between Jiaoye 1HF well and Woodford block

	Jiaoye 1HF well	One well in cana woodford field
Perforation mode	2 clusters of single-stage perforations with a diameter of 10.5 mm	3–6 clusters of single-stage perforations with a diameter of 14.5 mm
Fracturing fluid mode	Pretreatment acid + gel + slick water + gel	Pretreatment acid + linear gel + slick water + gel (high-viscosity fracturing fluid)

(Continued)

Table 5 (continued)

	Jiaoye 1HF well	One well in cana woodford field
Sanding method	Slug sanding with a low sand liquid ratio, the average comprehensive sand liquid ratio was 1.1%–4.2% (average 2.4%)	Continuous sanding with low sand liquid ratio, the average sand liquid ratio was 3%–6%
Liquid and sand volume	The fracturing fluid volume was 2460–3091 m^3, the average sand volume was 26–50 m^3	The fracturing fluid volume was 1800–2800 m^3, and the average sand volume was 80–110 m^3; single-stage fracturing operation was a large scale

5.1 Identification and Optimization of Comprehensive Vertical Dessert

The key to improving shale gas production capacity was the practical identification and comprehensive evaluation of reservoir dessert. We found many microscale structures in Southern Sichuan, and dessert strata were relatively thin in some areas. The southwest oil and gas field relied on foreign companies to provide rotary steerable tools and special drill bits for an ultra-long horizontal stage to increase the penetration rate of the targeted dessert layers [74]. The southwest oil and gas field commonly categorized the geological dessert in the following three ways (the first two were the most common, and the third was usually judged to be fracturing dessert): (1) the threshold values for geological dessert should be met at the same time: TOC > 3%, gas content > 2 m^3/t, and brittle mineral mass percent > 40%; (2) the geological dessert criteria had two main parts: the first was brittleness index and occurrence of shale gas, and the second was symbolic parameters affecting oil and gas-flow capacity, such as porosity, permeability, and saturation; (3) the geological dessert was characterized by the degree of reservoir fragmentation, which needed to satisfy the bedding and fracture index between 0.5 and 0.6, the brittleness index was between 0.55 and 0.6, and the fracture network propagation index was more significant than 0.6.

Based on the previous geological dessert and engineering dessert, this paper proposes the new evaluation method of the comprehensive vertical dessert of deep shale reservoir. The comprehensive vertical dessert of the shale reservoirs included geological, engineering, and fracturing desserts, which synthesized three factors: geology, engineering, and fracturing. The comprehensive dessert evaluation standards of shale reservoirs are shown in Fig. 7. The criteria for dividing geological dessert included factors affecting oil and gas enrichment, such as porosity, permeability, TOC, reservoir effective thickness, brittle mineral content, and hydrocarbon, oil, and gas saturation [75]. The evaluation standard for engineering dessert included factors affecting the matching between the horizontal well drilling technology penetration rate for a high-quality reservoirs, such as pinpointing horizontal well landing, a penetration rate of a high-quality reservoir, build-up rate, borehole curvature radius, horizontal well section length, well arrangement, and well spacing [76]. The judgment criteria for fracturing dessert were the key influencing factors of the fracturing network stimulations, including in situ stress information, brittleness index, compressibility, strength parameters, sand addition difficulty, weak surface (e.g., bedding and fractures), mineral filling degree, and stage spacing and spacing. Among these factors, the brittleness index reflected the features of the rock's mechanical parameters and the brittle mineral's content. Compressibility was defined as the ability to be effectively fractured

and increase production, which was the identification index used for early shale gas fracturing in China [77–79].

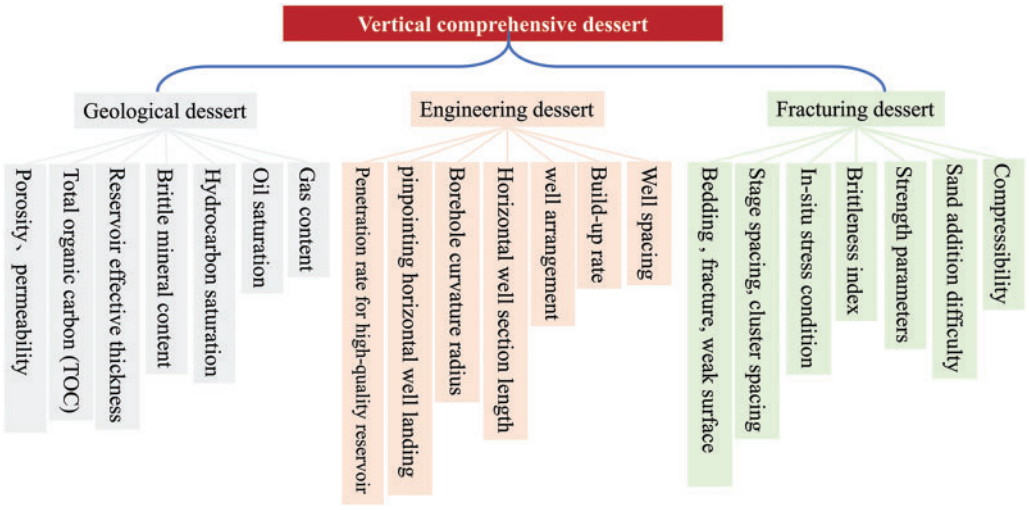

Figure 7: Evaluation criteria of comprehensive vertical dessert

To effectively improve the accuracy of vertical comprehensive dessert prediction, a series of methods, including geophysical exploration, reservoir characteristic evaluation, field, and laboratory experiments, could be adopted. Geophysical exploration, such as seismic prediction and logging, can be used to acquire three-dimensional geological models of shale reservoirs, reservoir structure, lithofacies information, and fault morphology. On this basis, reservoir thickness and spatial distribution could be made clear, and well trajectory also could be designed and better optimized. The reservoir classification standards and critical parameters of fracturing reconstruction could be obtained and combined with an evaluation of rock mechanical experiments, logging, and reservoir characteristics. Reservoir classification standards could be categorized as TOC, brittle mineral content, porosity, permeability and saturation, and fracturing reconstruction parameters included in-situ stress, brittleness, drillability, compressibility, Poisson's ratio, elastic modulus, and tensile strength.

5.2 Key Fracturing Stimulation Technologies

In China, early shale gas reservoirs were exploited mainly in shallow strata using conventional vertical fracturing stimulation. The key technical points included hydraulic sand-blasting perforation, annulus sand addition, and sand filling to plug the fractured stages. With the continuous development of horizontal well technology, China introduced horizontal well fracturing, horizontal well multistage/multicluster fracturing, simultaneous hydraulic fracturing, repeated fracturing, simultaneous fracturing, zipper fracturing, and "well factory" fracturing. Horizontal well multistage and multicluster fracturing technology is the primary technology used for shale gas fracturing at present. In 2013, BP Amoco conducted repeated fracturing on the first shale gas horizontal well D-1 in Woodford, and the production of well D-1 increased from 60×10^4 ft^3/d to 110×10^4 ft^3/d [80–82]. Repeated fracturing required more than 1000 applications in the United States. Simultaneous fracturing and zipper fracturing primarily relied on synchronous or asynchronous staged fracturing of two or more wells, which involved new fracturing methods under the "well factory" as well as the 3D-development mode of the requirements. These methods could be used to tremendously improve the development degree of the well fracture network and could expand the stimulated reservoir volume [27].

Based on the purpose of deep shale gas fracturing to improve the complexity of fracture network, increase the stimulated reservoir volume (SRV), and maintain the long-term conductivity of fractures, China changed its fracturing concept from "maximizing the SRV and complexity of fractures network" to "increasing the complexity of the fracture of near well formation and increasing the gas drainage area." [83–87]. At present, China has developed the critical technology for horizontal well large-scale and high-strength volume fracturing following the principle of "staged fracturing with dense cutting + shorter cluster spacing + fracture reorientation by pitching + forced-sand addition (sanding by large displacement and low-viscosity slick water) + increasing diameter perforating + proppant combination by high strength and small particle size particles." These comprehensive technologies could improve the effectiveness of fracture network stimulation, but the following characteristics are worthy of an in-depth study [88].

5.2.1 Staged Fracturing with Dense Cutting and Shorter Cluster Spacing

Currently, the standard techniques to improve the production of single shale gas wells have increased the number of fractures in the horizontal section and have shortened the fracture interval. These methods could enhance the stress shadow effect and could make the morphology of the fracture more complex through stress interference [89]. The well spacing was positively correlated with well-controlled reserves when the length of the horizontal section was certain. The controlled reserves of a single main hydraulic fracture became smaller when the stage spacing and cluster spacing were set rower. For the three-dimensional development of shale gas reservoirs, it was necessary to balance the relationship between the overall utilization degree of the gas reservoir and economic benefits [90–92]. The changes made to the horizontal well multistage/multicluster fracturing stimulation in the United States developed toward shorter stage length and rewer clusters. Taking the Haynesville field as an example, in 2011, the stage length was 90–120 m, and the cluster spacing was 20–30 m. The stage length and cluster spacing had been shortened year by year since 2012. In 2016, the stage length was 30–60 m, the cluster spacing was 6–15 m, and the temporary plugging and diverting generally were adopted for a stage length of 50–60 m.

To improve the fracturing effect for SRV and the fracture network complexity of deep shale gas reservoirs, China developed dense cluster and forced-sand addition technology based on the early multistage/multicluster fracturing technology, as shown in Table 6. Southern Sichuan adopted a combined fracturing fluid mode of "pretreated acid + gel fluid + slick water + gel fluid." The number of clusters increased from 3 to 5–11, the cluster spacing decreased from 25–30 m to 5–10 m, and the sand addition mass per unit length increased from 1.0–2.0 t/m to 2.5–3.0 t/m or higher. After employing the construction mode of "dense cutting stage + short cluster spacing distribution" in southern Sichuan's middle and deep strata, the production of a single well and estimated ultimate recovery (EUR) rate both improved. The test production of multiple wells exceeded 40×10^4 m^3/d, which illustrated that this construction had good adaptability in shale reservoirs with a high-stress difference in southern Sichuan. In addition, the perforation diameter was negatively correlated with the perforation friction under the same fluid injection conditions. Moderately increasing the perforation diameter effectively diminished the rock fracture pressure and reduced the fracturing construction difficulty. The dense cluster and forced-sand addition technologies were affected by the improved degree of perforating in different clusters (i.e., fracture and extension pressure). This could make it difficult for hydraulic fractures in each cluster to initiate and extend synchronously and could appear to be uneven fracture propagation. To control the equilibrium degree of fractures, it was necessary to cooperate with temporary plugging-in at the fracture mouth and nonuniform perforation.

Table 6: Evolution of shale reservoir fracturing stimulation parameters in China

Major operation parameter	Early	Current
Staged fracturing mode	Staged by quick drilling bridge plug + perforated by cable pumping	Staged by soluble bridge plug + perforated by cable pumping
Cluster number	2–3 (leading 3)	5–11
Cluster spacing/m	25–30	5–10
Stage length/m	60–80	60–80
Displacement/($m^3 \cdot min^{-1}$)	12–14	16–20
Sanding volume per unit length/($m^3 \cdot m^{-1}$)	30–40	25–30
Sanding mass per unit length/($t \cdot m^{-1}$)	1.0–2.0	2.5–3.0
Fracturing fluid type	Slick water	Variable viscosity slick water
Temporary plugging mode	Temporary plugging in fracture	Temporary plugging in fracture + temporary plugging in fracture mouth

5.2.2 Sanding Addition by Large Displacement and Low-Viscosity Slick Water

Deep shale formation had a high content of brittle minerals and an extensive brittleness index; therefore, it was appropriate to use low-viscosity slick water as the primary fracturing fluid to form a complex fracture network [93–95]. The net pressure was the key to generating a complex fracture network, and significant displacement of fracturing construction was the most direct and effective method to improve net pressure. The proppant would sediment rapidly under the influence of gravity when low-viscosity slick water and sand were used. Large displacement construction must be used to transport the proppant to the far end of the fracture, to achieve multistage support for branch fractures and microfractures. Large displacement construction also could increase the fracture width, help the proppant enter the formation through the fracture mouth, and reduce the risk of sand plugging. In addition, large displacement construction also minimized the lost risk caused by natural fracture filtration for the stratum with natural fractures [96]. In addition, perforation uses a particular perforating gun to shoot the casing, cement sheath, and part of the formation to create a flow channel for oil and gas for the wellbore and reservoir. Under these same injection conditions, the larger the perforation diameter, the larger the cross-sectional area of fracturing fluid flow, and the smaller the hole friction would be. Therefore, according to the universal understanding that "the higher the fracturing displacement, the better the flow limiting effect of perforations," increasing the construction displacement could give full play to the flow-limiting effect of perforations and could achieve multifracture opening and expansion when adopting big-hole perforating technology.

5.2.3 Proppant Combined with High-Strength and Small Particles

The horizontal principal stress difference of deep shale gas in Southwest China was significant, and the bottom hole closure pressure generally was more than 80 MPa. After the proppant entered

the fracture surface, the fracture conductivity would be reduced because of the embedding effect caused by the high closure stress. Therefore, a high-strength anticrushing proppant should be used. The embedding degree of proppant gradually increased with the decrease of pore pressure in the later stage of production, particularly after long-term contact between the fracture surface and the fracturing fluid and mud shale hydration. We identified several problems for deep shale gas well fracturing, such as easy sand plugging for fractures faces, complex sand addition, high Young's modulus of the reservoir, and limited width of slick water fracturing. To ensure the smooth passage of proppant through the fracture mouth and transportation in the fracture, a small particle size proppant should be used, and the laying concentration of proppant had to be increased. Generally, 70/140 mesh and 40/70 mesh combined proppant (the latter was the most common) were used for deep shale gas in southern Sichuan. In addition, considering the influence of factors, such as high closure stress, proppant embedding, proppant crushing, and the demand for fracture conductivity, more sand should be added when suitable conditions are available in the oil and gas fields. A big gap still existed between China and the United States in technologies, such as temporary plugging and diverting, high-density completion, and forced-sand addition [97–99].

5.2.4 Fracturing Fluid Optimization

The fracturing fluid cost of typical shale gas horizontal wells accounts for more than 30% of the total stimulation cost in China and the United States. The fracturing stimulation scale of horizontal wells was significant, equally "ten thousand cubic sand and ten thousand cubic fluids". Fracturing materials mainly included working fluid and proppant. The working fluid was pad fluid, carrying fluid, and displacement fluid, and the proppant was classified as silt, quartz sand, and ceramsite. Furthermore, the working fluid was compounded with a thickening agent, cleanup additive, antiswelling agent, temperature stabilizer, surface active agent, clay stabilizer, complexing agent, and crosslinking agent, with other additives under certain conditions. These auxiliary additives provided different effects for the fracturing fluid to stimulate operation. The buried depth of the shale gas reservoirs in the United States was relatively shallow. Horizontal wells were fractured primarily with "slick water + quartz sand." The compressive strength of U.S. quartz sand generally was higher than China's quartz sand. To maintain the fracture conductivity under the high closure pressure and horizontal principal stress differences in China's deep shale gas reservoir, it was necessary to use gel-liquids to improve the amount of sand added. The average gel-liquid ratio was 54%, though it was sometimes as high as 88%, and the average sanding mass per unit length was nearly 1.4 t/m. In addition, it was necessary to improve the sand-carrying capacity of the fracturing fluid and reduce its viscosity as much as possible. Therefore, based on optimizing drag reducer, drainage aid, tackifier material, and antiswelling agent, we found that slick water had the best characteristics, including instant solution, low viscosity, low friction, high antiswelling rate, and easy flow back [100]. The addition of slick water could change and redistribute the average velocity profile of the fracturing fluid. This redistributed the shear force in the boundary layer, which more effectively opened the natural fractures in the shale gas reservoir [101]. Under the development mode of long horizontal wells in the United States, Sinopec developed a staged fracturing design for long horizontal wells with the fine division of small layers, which was combined with brittleness and stress heterogeneity characteristics used in the sublayer in the Fuling shale gas field (see Table 7).

Table 7: Optimization of fractures parameters of Fuling sublayers

Stratum	Characteristic	Construction technology
Wufeng formation (I sublayer)	Bedding joints were well developed	Pre-gel + drag-reducing water, increasing the fracture length
Wufeng formation (III and IV sublayers)	Bedding joints were relatively developed	Drag-reducing water, increasing the fracture complexity
Wufeng formation (V sublayer)	Undeveloped fracture	Gel, increasing the fracture width; drag-reducing water, increasing the fracture complexity

5.2.5 Prevention of Interwell Interference

The development practice in the United States had proved that the application of the "well factory" fracturing greatly improved the fracturing construction speed, shortened the production cycle, and reduced gas production costs. The characteristics of "well factory" fracturing were as follows: the bottom sliding derricks were used to drill jungle well groups; each well group was composed of 3–8 single horizontal wells; and the spacing of the horizontal well was 300–400 m. These characteristics could maximize the coverage area of the shale development well and fracture multiple wells on a jungle well platform. It was easy for interwell interference to occur in the process of "well factory" fracturing. This interwell interference referred to the reservoir pressure and stress deficit induced by production during the development of low-permeability shale reservoirs and interference between adjacent horizontal wells caused by large-scale stimulation construction.

During simultaneous fracturing of two adjacent horizontal wells in the platform, fracturing fluid injection and rock fracture would lead to formation deformation and stress change. This stress shadow effect could affect the fracture propagation path and fracturing effect [102–104]. The stress shadow was directly related to the elastic parameters of the formation, the length and width of the expanding fractures, and the positional relationship between the existing fractures [105,106]. When performing dense-cutting staged hydraulic fracturing, the formation stress shadow could inhibit and change the initiation and propagation of new hydraulic fractures and also could increase the difficulty to generate a complex fracture network [107–109]. At the same time, the synchronous or asynchronous staged fracturing of two or more wells could induce the stress shadow effects and affect the shape of inter well-fracturing fracture networks.

Because the in situ stress state was an essential factor in controlling the propagation of hydraulic fracture networks, a deficit in old gas wells led to complex nonplanar fracture networks during infill of horizontal well fracturing and repeated fracturing. The interwell interference induced by horizontal infill wells and repeated fracturing occurred after the formation pressure and stress deficit caused by the production of gas wells. After the formation was deficient, the pore pressure decreased, and the magnitude and direction of the original in situ stress also changed considerably. In a state of complex in situ stress field, the heterogeneity of maximum principal stress, minimum principal stress, and horizontal stress difference was more robust, and the orientation of stress and hydraulic fracture also turned [110].

5.3 Staged Tools Development in Horizontal Wells

More than 85% of the horizontal wells fracturing in the United States used cementing operations for the casing. Pumping bridge plug was the leading technology used for fracturing stimulation, and open hole packer sliding sleeve fracturing also was applied relatively widely. The completion operation for mechanical casing packer mainly involved the combination of mechanical bridge plug and packer, control pressure by dual packer setting, and staged fracturing of the annular packer [111–113]. In addition, many oil companies also have been trying new fracturing-related technologies, such as perforation of the hydraulic sand blast, cementing operation for jungle sliding sleeve, and sliding-sleeve staged fracturing completion in casing cementing. The sliding-sleeve staged fracturing completion in casing cementing offered advantages such as unobstructed full borehole, no need for cable and coiled tubing, low cost, and high efficiency. The casing cementing staged fracture sliding sleeve included OptiPort, I-ball, ZoneSelect Monobore, FracPoint, and FSP™. At present, OptiPort and FSP™ have been put into field use in the United States. Staged tools included drillable composite bridge plug, large drift diameter bridge plug, soluble bridge plug, and frac ball seat (e.g., soluble ball seat and oversize drift diameter ball seat). Large foreign oil service companies, such as Schlumberger, Halliburton, Baker Hughes, Tryton, and Magnum, had developed and commercially applied a series of products, including soluble bridge plugs and frac ball sockets. Many oil fields and units, such as Southwest Oil and Gas Field, Changqing Oilfield, Chuanqing Drilling, and Jiebeitong, also have independently researched and commercially applied drillable composite bridge plugs and large drift diameter bridge plugs. Nevertheless, the fully soluble bridge plug remains in the experimental stage.

The well trajectory and formation dip angle in the deep shale reservoir were complex, and the coiled tubing drilling plug easily self-locked after fracturing. Therefore, it was difficult to drill and grind for the bridge plug and was not suitable for wholesale use to quickly drill a bridge plug. At present, the deep shale gas horizontal wells in Southwest China primarily employ high-temperature-resistant soluble bridge plugs. Simultaneously, to accelerate the dissolution rate of a soluble bridge plug, a cosolvent could be injected to ensure the complete dissolution of the soluble bridge plug and to shorten the oil-test cycle.

5.4 Fracture Network Morphology Monitoring

The two main kinds of fracture monitoring methods are microseismic and distributed optical fiber in petroleum engineering.

5.4.1 Microseismic Fracture Monitoring

Microseismic fracture monitoring was first used in the 1940 s. It was officially proposed in 1962 to corroborate the Kaiser effect for acoustic emission and had made tremendous developments in petroleum engineering. Microseismic monitoring was based on seismology, sound ballistics, elastic wave propagation and scattering theory, nonstationary signal analysis, rock mechanics, and computers. It was used to monitor and evaluate the fracturing effect by observing, collecting, and analyzing the microseismic events in fracturing construction. After the 1990 s, Canadian ESG, American Microseismic, Spectraseis, Schlumberger, Halliburton, French Magnitude, British Applied Seismology Consultants (ASC), and other oil companies could provide adequate technical support. At present, China depends primarily on the introduction of foreign technology and equipment.

When a large volume of fracturing fluid was pumped into the fracturing stimulation well, stress concentration would appear around the well. The microdeformation or microfracture propagation would occur in the original fracture or flow area when continuously pumped. The elastic strain energy

of the formation would be released in the form of a sound wave, that is, as microseismic events. Because the underground acoustic signal was weak and there was more noise on the ground, the microseismic receiver was generally underground about 304.8–914.4 m away from the fracturing well. Microseismic monitoring had the following two advantages:

Microseismic monitoring could assess the geometry and type of hydraulic fractures in real-time and could control the propagation of hydraulic fractures. It accurately determined SRV by monitoring and describing the specific position, magnitude, and strike in the propagation process of hydraulic fracturing [114,115], as shown in Fig. 8. Combined with reconstruction fracture morphology and SRV, it was convenient for the well sections that failed to be fully fractured to adjust the fracturing design scheme and to conduct repeated fracturing or temporary plugging and steering and further adapt the fracture trend. In addition, it could prevent hydraulic fractures from propagating to faults or aquifers and could avoid complex downhole accidents, such as leakage and water channeling [116,117].

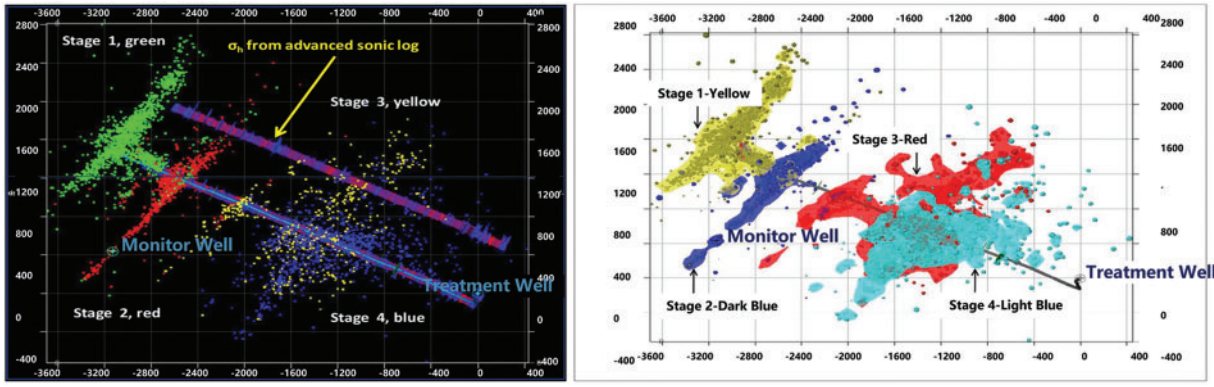

Figure 8: Microseismic reconstructed morphology and SRV during fracturing

Microseismic monitoring could inverse the mineral composition and in situ stress state of the stratum and judge the fracture type. The speed of the seismic wave in the reservoir could be inversed and combined with the seismic wave signal travel time. Then, the physical and mechanical parameters, such as reservoir quality, density, mineral composition, sand content, and porosity, could be inversed to predict oil and gas dessert and could guide well pattern arrangement. It also could fit the primary hydraulic fracture trend through microseismic event points to determine the direction of horizontal maximum/minimum principal stress and to provide convincing evidence for later deflecting, perforation, and fracturing design [118–120]. Ultimately, microseismic monitoring could be used to effectively judge the type of hydraulic fractures (tensile or shear) and focal mechanism (natural fracture opening, new fracture initiation, fault slip).

5.4.2 Distributed Optical Fiber Fracture Monitoring

Optical fiber offer the advantages of signal transmission stability, a large information capacity, high-temperature resistance, and disturbance-resistant solid ability. Distributed optical fiber can be categorized as distributed temperature sensing (DTS) and distributed acoustic sensing (DAS). Halliburton and Schlumberger of the United States and Silixa of the United Kingdom conducted systematic research on the theory and technology of distributed optical fiber monitoring systems and put these systems into use in oil fields. Less research has examined distributed optical fiber monitoring systems in China, and these systems have been used more often in the communication and construction industries.

DAS monitoring systems usually apply coherent optical time-domain reflectometry technology, which has been studied and applied less frequently in China, and also has been in its early stages in North America. Acoustic vibration can change the scattering position of the glass core on the microlevel of the optical cable, resulting in the transformation of the optical signal to form a series of independent acoustic signals. DAS systems can be used for downhole and regional monitoring, distributed flow measurement, sand production, and fracture monitoring [121–123]. The advantage of the DTS monitoring system is that it can clarify the relationship between temperature distribution and fluid properties, and its application is more mature than DAS.

DTS systems have been widely applied. They can be used to identify the change rate of fluid temperature, clarify the flow and distribution law of downhole fluid near the wellbore, determine the fracture location, predict the fluid flow distribution near the fracture, monitor the liquid output of the production well, and speculate the liquid production profile. Furthermore, Xinjiang Oilfield conducted temperature distribution for steam-assisted gravity drainage (SAGD) in the thermal recovery of heavy oil [124–126]. The DAS system had certain disadvantages in the three-dimensional spatial monitoring of fractures in the far well area. The DAS system should be combined with the injection point, perforation position, and fracture initiation position of the DTS system in the near-well area.

Distributed optical fiber usually analyzes the real-time data in the fracturing operation by optical fiber installed in the same or adjacent well. These data included the temperature/vibration of the fluid and the low-frequency signal generated by deformation. Hence, the same well monitoring could depict fracturing fluid and proppant distribution near each perforation cluster and fracturing stage. Clear DAS/DTS low-frequency strain and microseismic signals also could be received in the adjacent well. Adjacent well monitoring could be used to clearly describe the process of fracture initiation, propagation, and closure and analyze the phenomenon of adjacent well interference (fracture hits) [127,128], as shown in Fig. 9. Temporary optical fiber fracturing monitoring technology for adjacent wells significantly reduced the monitoring cost. This method also could be implemented simultaneously in multiple horizontal wells on the same platform to achieve omnidirectional and real-time monitoring.

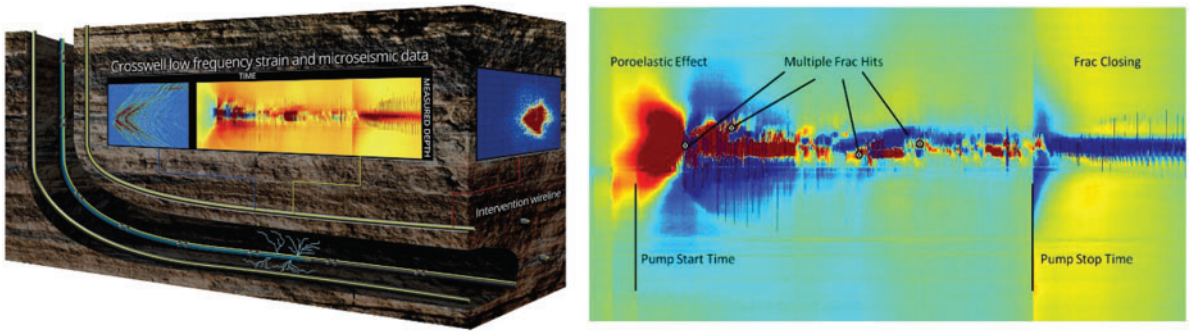

Figure 9: Optical fiber installed in adjacent well low-frequency strain during fracturing

5.5 Shale Hydration Expansion, Soak Well, and Fracturing Fluid Flow Back

The soak time of the shale gas well was referred to as the shut-in time from the completion of fracturing construction to the start of drilling plug. Combined with the experience of the Marcellus field in the United States, we found that soak well was conducive to the absorption of fracturing fluid for the shale matrix and enhanced the hydrophilicity of rock surface. This method also promoted the

desorption of free gas in microfractures and pores and in dredge pore channels, and also improved the relative permeability of the gas phase. The absorption of fracturing fluid by particles with a small matrix particle size and an increase in micropore water saturation was instrumental in displacing the gas phase to microfractures and macropores. The maturity of the organic matter also was closely positively related to productivity (except for soak time). Under the same soaking time, the higher the maturity of organic matter and the lower the clay content, the higher the productivity of gas wells [129–132].

The clay minerals dominated by illite and illite/montmorillonite mixed layer would create more microfractures after the hydration of fracturing fluid. The microfractures would extend and propagate with an increase in action time and finally could connect with the fracture network referring to the core micro-SEM experiment (Fig. 10). The hydration of the shale increased the liquid filtration area and gas-flow channel, reduced the flow-back rate of the fracturing fluid, and amplified the gas phase permeability. Hydration also could cut down the cohesion between mineral particles in shale, promote mineral dissolution and abscission, and finally produce more new microfracture groups [133]. Under this condition, the core stress weak point or weak surface increased, which provided more choices for the fracture initiation point and extension path.

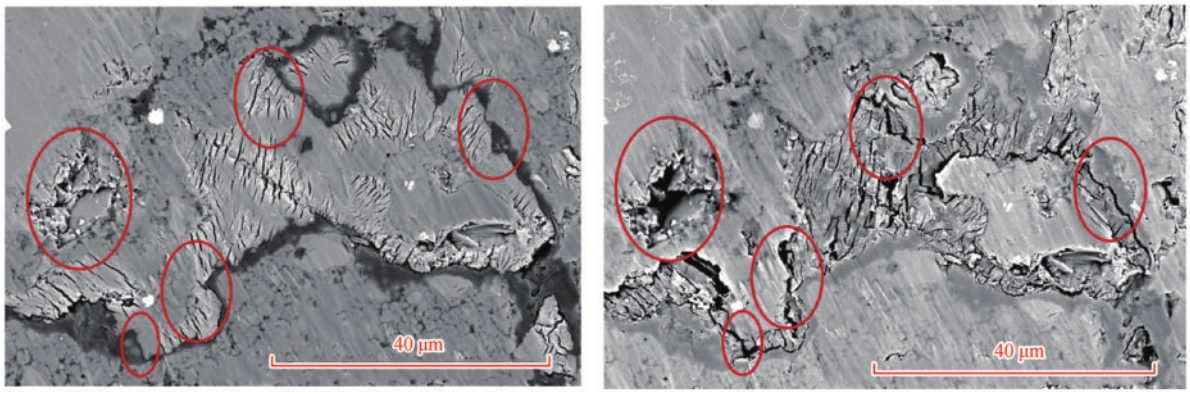

Figure 10: Comparison of SEM results of shale core before and after hydration

The soak time after volume fracturing of shale gas reservoir greatly influenced the fracturing effect and production. Under the action of capillary pressure and imbibition, the longer the soak time after fracturing, the more the fracturing fluid could fully realize oil-water replacement in the matrix, thus reducing the fracture water saturation and increasing the matrix water saturation. This change in the relative magnitude of saturation led to the concentration of shale gas around the fractures, thus shortening the flow-back period of the fracturing fluid. Some scholars have proposed shutting in the well for a few days or even months until most of the fracturing fluid could be absorbed by the shale [134–136]. Oil field practices, however, also showed that after the well was stewed for a specific time, the imbibition would reach an equilibrium state, and the oil-water replacement speed would slow down.

Moreover, a large amount of fracturing fluid retention easily caused damage to the reservoir. Even if the soaking time was prolonged, the shale gas production would not be significantly improved and could even reduce [137,138]. In addition to the shut-in time, the flow-back speed and flow-back mode also were important factors affecting the flow-back rate and production of the shale gas wells [139]. Referring to the statistics of 53 shale gas wells in the Longmaxi Formation of Changning field, we concluded that the microfractures of the shale reservoir always remained open during well soaking, and

a reasonable and optimal well soaking time was 5–10 days. The "slow blowback mode" was successfully used in Haynesville, Eagle Ford, and other oil fields, and the ultimate recovery was increased by about 5% [140]. On this basis, the flow-back mode of "nozzle control, step-by-step amplification, continuous, and stable" was adopted in southern Sichuan at the initial stage of the drilling plug [141].

The flow-back fluid referred to the solid-liquid-gas mixture (mainly liquid) that flowed back to the ground after the drilling plug, including the shale gas in the wellbore, fracturing fluid, and proppant, which that did not play a supporting role [142,143]. The flow-back period generally lasted from several days to several weeks, and the latter stage mainly included a small amount of fracturing fluid and plenty of formation water. Fracturing fluid flow back had three phases, as shown in Fig. 11. In Phase I, the flow-back mixture at the initial stage of well opening was mainly a solid-liquid mixture, including scattered proppant, suspended solid particles, and polymer residue. In Phase II, as the fracturing fluid was discharged, the reservoir pressure would decrease, and the proppant began to embed into the fracture surface. Meanwhile, the adsorbed gas on the matrix and pore surface also started to desorb and diffuse into the hydraulic fracture. Simultaneously, the flow-back liquid was a solid-liquid-gas three-phase mixture, the mutual adhesion force between proppants was weakened, the gravel would migrate, and the relative permeability of gas-phase would increase. In Phase III, the water phase in the retained fracturing fluid gradually evaporated when all of the fracturing fluid flowed back, which was accompanied by soluble salt precipitation. Furthermore, the decrease in reservoir pressure would lead to the deeper insertion of proppant gravel into the fracture surface.

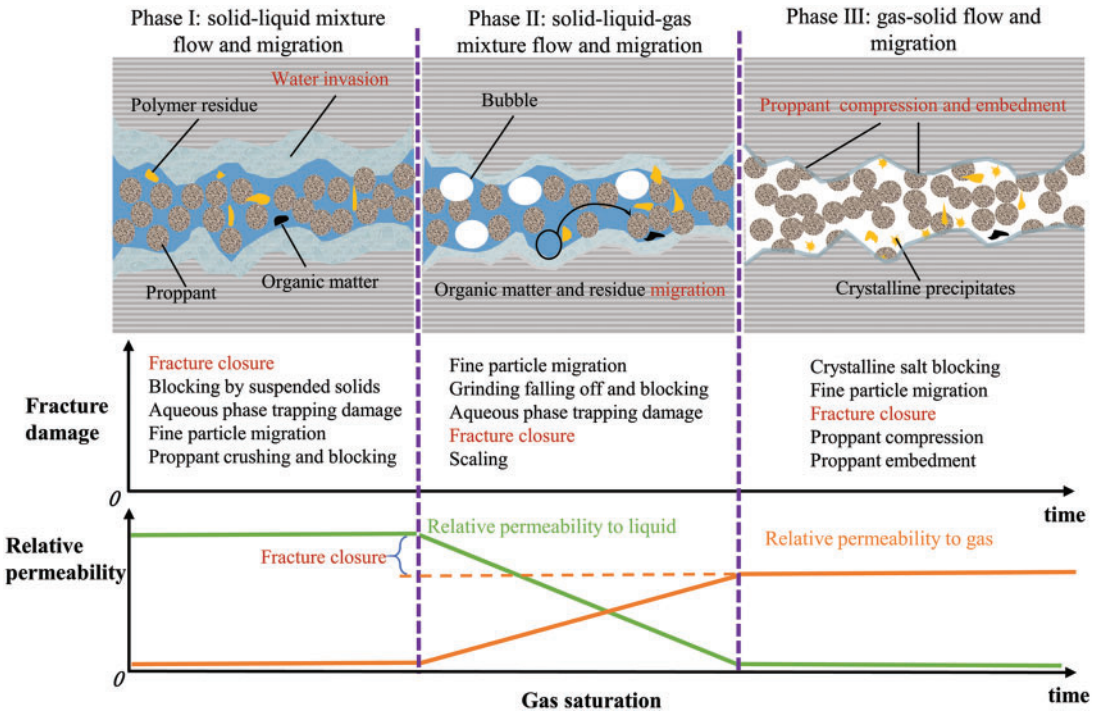

Figure 11: Schematic diagram of fracturing fluid flow back

6 Development Prospects of Shale Gas Fracturing in China

6.1 Deep and Ultra-Deep Marine Shale Gas Fracturing

The core contradictions of deep and ultra-deep shale gas fracturing are reflected in three main aspects: (1) The cost of shaft construction and fracturing stimulation of deep shale gas reservoirs is high. The overall trial production is low and there is a severe contradiction in economic development. (2) The threshold production of deep shale gas reservoirs to achieve economic development is high; it needs a more developed discrete fracture network. However, the geomechanical properties of deep shale gas reservoirs causes a severe inhibitory effect on the construction of fracture networks. A sharp contradiction exists between the high demand for fracture networks and the difficulty of creating these networks. (3) The closing pressure of deep shale formation is high, and it is necessary to inject proppant with higher concentrations and larger particles to realize the effective support of hydraulic fractures. The in situ stress and mechanical properties, however, lead to a small fracture width. This contradiction between the effective support of the fracture network and the difficulty in proppant injection is prominent. Because of these essential differences in fracture network stimulation technology between deep and ultra-deep reservoirs and medium and shallow stratum, the basic theory and technology of fracturing stimulation for deep and ultra-deep reservoirs must be established and developed.

6.2 Hydraulic Fracturing of Marine-Continental Facies Shale Reservoirs

China's shale gas resources marine-continental facies rank high globally and possess significant exploration and development prospects. The quantity is about 19.8×10^{12} m^3, accounting for 25% of domestic shale gas resources. China's reservoirs have multiple overlapping strata, including coal, dense sandstone, and limestone. Thus, fracturing stimulation technology faces a series of challenges: (1) The thickness of a single layer is thin, the interaction effects of thin layers are significant, and the rock deformation characteristics and failure mode are different from those of marine shale. (2) The reservoir lithofacies change rapidly and assemble multiply. Therefore, the deflection extension of the hydraulic fracture network passing through the lithologic interface is complex. (3) The reservoir pressure coefficient is relatively low, and the formation sensitivity of different lithologies is different. (4) The reservoir has substantial heterogeneity and significant vertical and horizontal lithology changes, making it difficult for multilayer fracturing stimulation. Because the fracturing stimulation technology of marine-continental facies has not been well established, it is urgent to conduct correlative system research.

6.3 Advocating Anhydrous Fracturing

Insufficient water resources and weak environmental protection are essential problems faced by shale gas exploitation in China. At the same time, with the development of marine and marine-continental facies shale, the water-based fracturing fluid system not only consumes an excessive amount of water resources but also has poor adaptability and stimulation effects on the reservoirs. Shale gas exploitation offers broad prospects to make full use of the advantages of the excellent compatibility between anhydrous fracturing fluid systems, such as CO_2 and N_2, and formation fluid.

6.4 Research and Development of Crucial Fracturing Tools

The staged fracturing tools, such as bridge plugs and cemented sliding sleeves, have been partially localized. They still face challenges in deep and ultra-deep shale's high-temperature and high-stress environment. The manufacture and independent production of precision downhole tools have become troublesome issues in the efficient development of shale gas. It would be best to speed up the development of the key tools necessary for shale gas fracturing and realize localization and

serialization. For example, it is necessary to promote domestic cementing sliding sleeve tools and tackle fundamental problems to make their temperature resistance exceed 200°C.

6.5 High-Efficiency Exploitation Technology of Adsorbed Gas

In the main shale gas-producing areas in the United States, the proportion of adsorbed gas in the total gas volume is less than 35%. The ratio of adsorbed gas in the Jiaoshiba and Changning regions in China accounts for more than 40%. The shale reservoirs in China are buried deeper and develop more natural fractures. Therefore, the construction of the hydraulic fracture network is more complicated; the propagation of pressure drop in the reservoir is significantly restrained. Many of the adsorbed gases stored in deep reservoirs cannot be affected by pressure drop, making it challenging to form efficient desorption. Therefore, it is necessary to adopt CO_2 replacement, controllable shock wave, high-temperature heat treatment, oxidative decomposition, and acoustic electromagnetic to promote the rapid desorption of adsorbed gas and realize the economic and efficient development of shale gas [144–146].

7 Conclusions

This study first compared the development history of shale gas and mechanical and physical parameters of deep and shallow reservoirs in the United States and China. Combined with the advanced technology systems, stage tools development, and supporting technologies in shale gas exploration and development in the United States, the following ideas could enhance China's deep shale gas development:

1. The order-of-magnitude difference between China's output and the annual output of shale gas in the United States could be attributed to three main factors: reservoir buried depth, reservoir physical and mechanical properties, and engineering technology level. The buried depth of shale gas reservoirs in the United States ranged from 1200 to 4500 m, most of which were medium and shallow layers, with porosity spanning from 1% to 12% and matrix permeability changing from 0.001 to 2 mD. The buried depth of shale in the Sichuan Basin in China was 800–5900 m, most of which were concentrated in the middle and deep layers. The maximum porosity was only 8%, with an average of 1.65%–4.52%, and the permeability range was 0.029–0.77 mD. The porosity and permeability parameters and physical property indexes of shale reservoirs in the United States were higher than those in China.
2. Deep shale reservoirs featured several characteristics, including the development of bedding fracture, low brittleness index, and low clay mineral content, and had significant areal differences, including the transformation from elasticity to plasticity, difficulty in the sanding, and high mechanical and strength parameters. Moreover, these reservoirs also had six high values of formation temperature, horizontal principal stress difference, pore pressure, fracture pressure, extension pressure, and closure pressure. These six characteristics led to a higher threshold of production for horizontal drilling and fracturing in the deep shale reservoirs.
3. China initially formed the critical technology of horizontal well large-scale and high-strength volume fracturing following the core of "staged fracturing with dense cutting + shorter cluster spacing + fracture reorientation by pitching + forced-sand addition (sanding by large displacement and low-viscosity slick water) + increasing diameter perforating + proppant combination by high strength and small particle size particles". China can continue to carry out critical research on theories and technical methods of horizontal well fracturing, suitable

for domestic deep and ultra-deep marine and marine-continental sedimentary shale, to support and promote the efficient development of shale gas in China in the future.

4. Microseismic, DTS, and DAS monitoring methods could complement each other in shale oil and gas and tight oil and gas production. DTS and DAS could transmit temperature, pressure, acoustic wave, and other data in real-time by tubing conveyed and temporary fixing, which offer significant engineering guidance to judge downhole complex accidents.
5. It was necessary to balance the relationship between the overall utilization degree of the gas reservoir and economic benefits. The development of deep shale gas required a longer horizontal stage length and a larger fracturing scale, and thus the single-well cost was higher. The current single-well production and EUR were low, and some essential tools and supporting technologies were not localized. Therefore, it was challenging to meet the economic requirements for deep shale reservoirs.

Funding Statement: This research is funded by the National Key Research and Development Program of China under Grant No. 2020YFC1808102, the National Natural Science Foundation of China (Grant Nos. 51874328, U1762215), and the Strategic Cooperation Technology Projects of CNPC and CUPB (Grant No. ZLZX2020-02).

Conflicts of Interest: The authors declare that they have no conflicts of interest to report regarding the present study.

References

1. Curtis, M. E., Ambrose, R. J., Sondergeld, C. H., Rai, C. S. (2011). Transmission and scanning electron microscopy investigation of pore connectivity of gas shales on the nanoscale. *North American Unconventional Gas Conference and Exhibition*, The Woodlands, Texas, USA. DOI 10.2118/144391-ms.
2. Xia, L. W., Cao, J., Wang, M., Mi, J. L., Wang, T. T. (2019). A review of carbonates as hydrocarbon source rocks, basic geochemistry and oil–gas generation. *Petroleum Science, 16(4),* 713–728. DOI 10.1007/s12182-019-0343-5.
3. Zhou, Z., Slaný, M., Kuzielová, E., Zhang, W., Ma, L. et al. (2022). Influence of reservoir minerals and ethanol on catalytic aquathermolysis of heavy oil. *Fuel, 307,* 121871. DOI 10.1016/j.fuel.2021.121871.
4. Keller, J. U., Dreisbach, F., Rave, H., Staudt, R., Tomalla, M. (1999). Measurement of gas mixture adsorption equilibria of natural gas compounds on microporous sorbents. *Adsorption, 5(3),* 199–214. DOI 10.1023/A:1008998117996.
5. Jarvie, D. M., Hill, R. J., Ruble, T. E., Pollastro, R. M. (2007). Unconventional shale-gas systems, the mississippian barnett shale of North-Central Texas as one model for thermogenic shale-gas assessment. *AAPG Bulletin, 91(4),* 475–499. DOI 10.1306/12190606068.
6. Shi, J., Zhang, L., Li, Y., Yu, W., He, X. et al. (2013). Diffusion and flow mechanisms of shale gas through matrix pores and gas production forecasting. *SPE Unconventional Resources Conference*, Canada.
7. Gasparik, M., Gensterblum, Y., Ghanizadeh, A., Weniger, P., Krooss, B. M. (2015). High-pressure/high-temperature methane-sorption measurements on carbonaceous shales by the manometric method, experimental and data-evaluation considerations for improved accuracy. *SPE Journal, 20(4),* 790–809. DOI 10.2118/174543-PA.
8. Hildenbrand, A., Krooss, B. M., Busch, A., Gaschnitz, R. (2006). Evolution of methane sorption capacity of coal seams as a function of burial history—A case study from the campine basin, NE Belgium. *International Journal of Coal Geology, 66(3),* 179–203. DOI 10.1016/j.coal.2005.07.006.

9. Jin, J., Jin, Y., Lu, Y., Pang, H. (2022). Image processing and machine learning based cavings characterization and classification. *Journal of Petroleum Science and Engineering, 208,* 109525. DOI 10.1016/j.petrol.2021.109525.
10. Yao, Y., Ge, J. (2011). Characteristics of non-darcy flow in low-permeability reservoirs. *Petroleum Science, 8(1),* 55–62. DOI 10.1007/s12182-011-0115-3.
11. Fan, T., Zhang, G., Cui, J. (2014). The impact of cleats on hydraulic fracture initiation and propagation in coal seams. *Petroleum Science, 11(4),* 532–539. DOI 10.1007/s12182-014-0369-7.
12. Zhang, H., Li, T., Han, D., Wang, D., Sun, D. et al. (2020). Study on a dual embedded discrete fracture model for fluid flow in fractured porous media. *Computer Modeling in Engineering & Sciences, 124(1),* 5–21. DOI 10.32604/cmes.2020.09290.
13. Devloo, P., Teng, W., Zhang, C. S. (2019). Multiscale hybrid-mixed finite element method for flow simulation in fractured porous media. *Computer Modeling in Engineering & Sciences, 119(1),* 145–163. DOI 10.32604/cmes.2019.04812.
14. Micheal, M., Xu, W., Xu, H., Zhang, J., Jin, H. et al. (2021). Multi-scale modelling of gas transport and production evaluation in shale reservoir considering crisscrossing fractures. *Journal of Natural Gas Science and Engineering, 95,* 104156. DOI 10.1016/j.jngse.2021.104156.
15. Liu, C., Shen, Y., Zhang, J., Lu, D., Liu, H. et al. (2019). Production analysis in shale gas reservoirs based on fracturing-enhanced permeability areas. *Science China Physics*, *Mechanics & Astronomy, 62(10),* 1–9. DOI 10.1007/s11433-019-9427-x.
16. Yu, H., Xu, H., Fan, J., Zhu, Y. B., Wang, F. et al. (2020). Transport of shale gas in microporous/nanoporous media, molecular to pore-scale simulations. *Energy & Fuels, 35(2),* 911–943. DOI 10.1021/acs.energyfuels.0c03276.
17. Weijermars, R., Sorek, N., Sen, D., Ayers, W. B. (2017). Eagle Ford Shale play economics, U.S. versus Mexico. *Journal of Natural Gas Science and Engineering, 38,* 345–372. DOI 10.1016/j.jngse.2016.12.009.
18. Kerr, R. A. (2010). Natural gas from shale bursts onto the scene. *Science, 328(5986),* 1624–1626. DOI 10.1126/science.328.5986.1624.
19. Mayerhofer, M. J., Richardson, M. F., Walker, R. N., Meehan, D. N., Oehler, M. W. et al. (1997). Proppants? We don't need no proppants. *SPE Annual Technical Conference and Exhibition*, San Antonio, Texas, USA. DOI 10.2118/38611-MS.
20. Gupta, A., Gupta, A., Langlinais, J. (2005). Feasibility of supercritical carbon dioxide as a drilling fluid for deep underbalanced drilling operation. *Proceedings of SPE Annual Technical Conference and Exhibition*, Dallas, Texas, USA. DOI 10.2523/96992-ms.
21. Meng, S., Liu, H., Xu, J., Duan, Y., Yang, Q. et al. (2016). The evolution and control of fluid phase during liquid CO_2 fracturing. *SPE Asia Pacific Hydraulic Fracturing Conference*, Beijing, China. DOI 10.2118/181790-ms.
22. Wamock, W. E., Harris, P. C., King, D. S. (1985). Successful field applications of CO_2-foam fracturing fluids in the Arkansas-Louisiana-Texas region. *Journal of Petroleum Technology, 37(1),* 80–88. DOI 10.2118/11932-pa.
23. Soni, T. M. (2014). LPG-Based fracturing: An alternate fracturing technique in shale reservoirs. *IADC/SPE Asia Pacific Drilling Technology Conference*, Bangkok, Thailand. DOI 10.2118/170542-ms.
24. Freeman, D. L., Bush, D. C. (1983). Low-permeability laboratory measurements by nonsteady-state and conventional methods. *Society of Petroleum Engineers Journal, 23(6),* 928–936. DOI 10.2118/10075-pa.
25. Ketter, A. A., Daniels, J. L., Heinze, J. R., Waters, G. (2008). A field study in optimizing completion strategies for fracture initiation in barnett shale horizontal wells. *SPE Production & Operations, 23(3),* 373–378. DOI 10.2118/103232-pa.
26. Gupta, J., Zielonka, M., Albert, R. A., El-Rabaa, A. M., Burnham, H. A. et al. (2012). Integrated methodology for optimizing development of unconventional gas resources. *SPE Hydraulic Fracturing Technology Conference*, The Woodlands, Texas, USA. DOI 10.2118/152224-ms.

27. Rafiee, M., Soliman, M. Y., Pirayesh, E. (2012). Hydraulic fracturing design and optimization: A modification to zipper frac. *SPE Annual Technical Conference and Exhibition*, San Antonio, Texas, USA. DOI 10.2118/159786-ms.
28. Liang, B., Du, M., Yanez, P. P. (2019). Subsurface well spacing optimization in the Permian Basin. *Journal of Petroleum Science and Engineering, 174,* 235–243. DOI 10.15530/urtec-2017-2671346.
29. Patel, H., Cadwallader, S., Wampler, J. (2016). Zipper fracturing, taking theory to reality in the eagle ford shale. *Unconventional Resources Technology Conference*, pp. 1000–1008. San Antonio, Texas.
30. Rutqvist, J., Rinaldi, A. P., Cappa, F., Moridis, G. J. (2015). Modeling of fault activation and seismicity by injection directly into a fault zone associated with hydraulic fracturing of shale-gas reservoirs. *Journal of Petroleum Science and Engineering, 127,* 377–386. DOI 10.1016/j.petrol.2015.01.019.
31. Rahm, D. (2011). Regulating hydraulic fracturing in shale gas plays, the case of texas. *Energy Policy, 39(5),* 2974–2981. DOI 10.1016/j.enpol.2011.03.009.
32. Arthur, J. D., Bohm, B. K., Coughlin, B. J., Layne, M. A., Cornue, D. (2009). Evaluating the environmental implications of hydraulic fracturing in shale gas reservoirs. *SPE Americas E&P Environmental and Safety Conference*, San Antonio, Texas, USA. DOI 10.2118/121038-ms.
33. Vengosh, A., Jackson, R. B., Warner, N., Darrah, T. H., Kondash, A. (2014). A critical review of the risks to water resources from unconventional shale gas development and hydraulic fracturing in the United States. *Environmental Science & Technology, 48(15),* 8334–8348. DOI 10.1021/es405118y.
34. Sovacool, B. K. (2014). Cornucopia or curse? reviewing the costs and benefits of shale gas hydraulic fracturing (fracking). *Renewable and Sustainable Energy Reviews, 37,* 249–264. DOI 10.1016/j.rser.2014.04.068.
35. Estrada, J. M., Bhamidimarri, R. (2016). A review of the issues and treatment options for wastewater from shale gas extraction by hydraulic fracturing. *Fuel, 182,* 292–303. DOI 10.1016/j.fuel.2016.05.051.
36. Zhao, J., Ren, L., Jiang, T., Hu, D., Wu, L. et al. (2021). Ten years of shale gas fracturing in China, review and prospect. *Natural Gas Industry, 41(8),* 121–142. DOI 10.3787/j.issn.1000-0976.2021.08.012.
37. Jia, C. Z., Pang, X. Q., Jiang F, J. (2016). Research status and development directions of hydrocarbon resources in China. *Petroleum Science Bulletin, 1(1),* 2–23. DOI 10.3969/j.issn.2096-1693.2016.01.001.
38. Zeng, Y. J. (2019). Progress in engineering technologies for the development of deep shale gas. *Petroleum Science Bulletin, 3,* 233–241. DOI 10.3969/j.issn.2096-1693.2019.03.021.
39. Hou, B., Chang, Z., Fu, W., Muhadasi, Y., Chen, M. (2019). Fracture initiation and propagation in a deep shale gas reservoir subject to an alternating-fluid-injection hydraulic-fracturing treatment. *SPE Journal, 24(4),* 1839–1855. DOI 10.2118/195571-pa.
40. Hou, B., Diao, C., Li, D. (2017). An experimental investigation of geomechanical properties of deep tight gas reservoirs. *Journal of Natural Gas Science and Engineering, 47,* 22–33. DOI 10.1016/j.jngse.2017.09.004.
41. Hou, B., Zhang, R., Chen, M., Kao, J., Liu, X. (2019). Investigation on acid fracturing treatment in limestone formation based on true tri-axial experiment. *Fuel, 235,* 473–484. DOI 10.1016/j.fuel.2018.08.057.
42. Hou, B., Cui, Z., Ding, J. H., Zhang, F. S., Zhuang, L. et al. (2022). Perforation optimization of layer-penetration fracturing for commingling gas production in coal measure strata. *Petroleum Science*. DOI 10.1016/j.petsci.2022.03.014.
43. Wang, H., Shi, Z., Sun, S., Zhang, L. (2021). Characteristics and genesis of deep shale reservoirs in the first member of silurian longmaxi formation in Sichuan Basin and its periphery. *Petroleum and Natural Gas Geology, 42 (1),* 66–75. DOI 10.11743/ogg20210106.
44. Zeng, Y., Chen, Z., Bian, X. (2016). Breakthrough in staged fracturing technology for deep shale gas reservoirs in SE Sichuan Basin and its implications. *Natural Gas Industry B, 3(1),* 45–51. DOI 10.1016/j.ngib.2016.02.005.
45. Shan, Q., Jin, Y., Chen, M., Yang, S., Zhang, X. et al. (2015). Causes of and responses to abnormal fracture pressure on ultra-deep shale in Southern China. *SPE Asia Pacific Unconventional Resources Conference and Exhibition*, Brisbane, Australia. DOI 10.2118/176951-ms.

46. Zhang, Y., Gao, S., Du, X., Chen, M., Jin, Y. (2019). Molecular dynamics simulation of strength weakening mechanism of deep shale. *Journal of Petroleum Science and Engineering, 181,* 106123. DOI 10.1016/j.petrol.2019.05.074.
47. Zhang, Q., Lin, B., Kao, J., Chen, A., Shi, S. et al. (2020). Characterization of stress field around a reverse fault based on a constraint stress model. *54th US Rock Mechanics/Geomechanics Symposium*. OnePetro (Physical Event Cancelled).
48. Wan, L., Hou, B., Tan, P., Chang, Z., Muhadasi, Y. (2019). Observing the effects of transition zone properties on fracture vertical propagation behavior for coal measure strata. *Journal of Structural Geology, 126,* 69–82. DOI 10.1016/j.jsg.2019.05.005.
49. Hou, B., Chen, M., Wang, Z., Yuan, J., Liu, M. (2013). Hydraulic fracture initiation theory for a horizontal well in a coal seam. *Petroleum Science, 10(2),* 219–225. DOI 10.1007/s12182-013-0270-9.
50. Tan, P., Jin, Y., Yuan, L., Xiong, Z. Y., Hou, B. et al. (2019). Understanding hydraulic fracture propagation behavior in tight sandstone–coal interbedded formations, an experimental investigation. *Petroleum Science, 16(1),* 148–160. DOI 10.1007/s12182-018-0297-z.
51. Cheng, Z., Wang, Z., Luo, Z. (2019). Dynamic fracture analysis for shale material by peridynamic modelling. *Computer Modeling in Engineering & Sciences, 118(3),* 509–527. DOI 10.31614/cmes.2019.04339.
52. Wang, Y., Hou, B., Zhang, K., Zhou, C., Liu, F. (2020). Laboratory true triaxial acid fracturing experiments for carbonate reservoirs. *Petroleum Science Bulletin, 3,* 412–419. DOI 10.3969/j.issn.2096-1693.2020.03.035.
53. Hou, B., Chang, Z., Wu, A., Elsworth, D. (2022). Simulation of competitive propagation of multi-fractures on shale oil reservoir multi-clustered fracturing in Jimsar sag. *Acta Petrolei Sinica, 43(1),* 75. DOI 10.7623/syxb202201007.
54. Li, Y. (2021). Mechanics and fracturing techniques of deep shale from the Sichuan Basin, SW China. *Energy Geoscience, 2(1),* 1–9. DOI 10.1016/j.engeos.2020.06.002.
55. Ma, X., Wang, H., Zhou, S., Shi, Z., Zhang, L. (2021). Deep shale gas in China, geological characteristics and development strategies. *Energy Reports, 7,* 1903–1914. DOI 10.1016/j.egyr.2021.03.043.
56. Gou, Q., Xu, S. (2019). Quantitative evaluation of free gas and adsorbed gas content of Wufeng-Longmaxi shales in the Jiaoshiba area, Sichuan Basin, China. *Advances in Geo-Energy Research, 3(3),* 258–267. DOI 10.26804/ager.
57. Zhou, S., Ning, Y., Wang, H., Liu, H., Xue, H. (2018). Investigation of methane adsorption mechanism on Longmaxi shale by combining the micropore filling and monolayer coverage theories. *Advances in Geo-Energy Research, 2(3),* 269–281. DOI 10.26804/ager.
58. Ibanez, W. D., Kronenberg, A. K. (1993). Experimental deformation of shale, mechanical properties and microstructural indicators of mechanisms. *International Journal of Rock Mechanics and Mining Sciences & Geomechanics Abstracts, 30(7),* 723–734. DOI 10.1016/0148-9062(93)90014-5.
59. Valès, F., Minh, D. N., Gharbi, H., Rejeb, A. (2004). Experimental study of the influence of the degree of saturation on physical and mechanical properties in tournemire shale (France). *Applied Clay Science, 26(1–4),* 197–207. DOI 10.1016/j.clay.2003.12.032.
60. Guan, X., Yi, X., Yang, H. (2014). Contrast of shale gas reservoir conditions in China and the United States. *Journal of Southwest Petroleum University, Science & Technology Edition, 36(5),* 33–39. DOI 10.11885/j.issn.1674-5086.2013.12.05.01.
61. Amann, F., Button, E. A., Evans, K. F., Gischig, V. S., Blümel, M. (2011). Experimental study of the brittle behavior of clay shale in rapid unconfined compression. *Rock Mechanics and Rock Engineering, 44(4),* 415–430. DOI 10.1007/s00603-011-0156-3.
62. Amann, F., Kaiser, P., Button, E. A. (2012). Experimental study of brittle behavior of clay shale in rapid triaxial compression. *Rock Mechanics and Rock Engineering, 45(1),* 21–33. DOI 10.1007/s00603-011-0195-9.
63. Eseme, E., Urai, J. L., Krooss, B. M., Littke, R. (2007). Review of mechanical properties of oil shales, impactions for exploitation and basin modeling. *Oil Shale, 24(2),* 159–174. DOI 10.3176/oil.2007.2.06.

64. Niandou, H., Shao, J. F., Henry, J. P., Fourmaintraux, D. (1997). Laboratory investigation of the mechanical behaviour of tournemire shale. *International Journal of Rock Mechanics and Mining Sciences, 34(1),* 3–16. DOI 10.1016/S1365-1609(97)80029-9.

65. Curtis, J. B. (2002). Fractured shale-gas systems. *AAPG Bulletin, 86(11),* 1921–1938.

66. Tang, Y., Slaný, M., Yang, Y., Li, S., Qin, F. et al. (2022). Highly active Mg–Al hydrotalcite for efficient O-methylation of phenol with DMC based on soft colloidal templates. *Journal of Chemical Technology & Biotechnology, 97(1),* 79–86. DOI 10.1002/jctb.6912.

67. Ross D, J. K., Bustin R, M. (2007). Shale gas potential of the lower jurassic gordondale member, Northeastern British Columbia, Canada. *Bulletin of Canadian Petroleum Geology, 55(1),* 51–75. DOI 10.2113/gscpgbull.55.1.51.

68. Sondergeld, C. H., Newsham, K. E., Comisky, J. T., Rice, M. C., Rai, C. S. (2010). Petrophysical considerations in evaluating and producing shale Gas resources. *SPE Unconventional gas Conference*, Pittsburgh, Pennsylvania, USA. DOI 10.2118/131768-ms.

69. Islam M, A., Skalle, P. (2013). An experimental investigation of shale mechanical properties through drained and undrained test mechanisms. *Rock Mechanics and Rock Engineering, 46(6),* 1391–1413. DOI 10.1007/s00603-013-0377-8.

70. Wei, Y., Anand, L. (2008). On micro-cracking, inelastic dilatancy, and the brittle-ductile transition in compact rocks: A micro-mechanical study. *International Journal of Solids and Structures, 45(10),* 2785–2798. DOI 10.1016/j.ijsolstr.2007.11.028.

71. Shi, C., Lin, B. (2021). Principles and influencing factors for shale formations. *Petroleum Science Bulletin, 1,* 92–113. DOI 10.3969/j.issn.2096-1693.2021.01.008.

72. Rybacki, E., Reinicke, A., Meier, T., Makasi, M., Dresen, G. (2015). What controls the mechanical properties of shale rocks?–Part I, strength and Young's modulus. *Journal of Petroleum Science and Engineering, 135,* 702–722. DOI 10.1016/j.petrol.2015.10.028.

73. Rybacki, E., Meier, T., Dresen, G. (2016). What controls the mechanical properties of shale rocks?–Part II, brittleness. *Journal of Petroleum Science and Engineering, 144,* 39–58. DOI 10.1016/j.petrol.2016.02.022.

74. Zhao, C. S., Wan, H., Zhang, H., Zhang, J. L., Pan, X. Z. et al. (2019). Research application of the P-wave anisotropy forward modeling and pre-stack fracture detection, take the tight sandstone gas block in Ordos Basin as an example. *Progress in Geophysics, 34(1),* 257–265. DOI 10.6038/pg2019BB0472.

75. Zhang, W., Slaný, M., Zhang, J., Liu, Y., Zang, Y. et al. (2021). Acetylation modification of waste polystyrene and Its Use as a crude Oil flow improver. *Polymers, 13(15),* 2505. DOI 10.3390/polym13152505.

76. Yu, B., Yan, C., Gao, D., Li, J. (2012). A study on the stability of the borehole in shale, in extended-reach drilling. *Computer Modeling in Engineering & Sciences, 89(1),* 57–78. DOI 10.3970/cmes.2012.089.057.

77. Ruddy, I., Andersen, M. A., Pattillo, P. D., Bishlawi, M., Foged, N. (1989). Rock compressibility, compaction, and subsidence in a high-porosity chalk reservoir: A case study of valhall field. *Journal of Petroleum Technology, 41(7),* 741–746. DOI 10.2118/18278-PA.

78. Chong, K. K., Grieser, W. V., Passman, A., Tamayo, C. H., Modeland, N. et al. (2010). A completions guide book to shale-play development: A review of successful approaches towards shale-play stimulation in the last two decades. *Canadian Unconventional Resources and International Petroleum Conference*, Calgary, Alberta, Canada. DOI 10.2118/133874-MS.

79. Bai, M. (2016). Why are brittleness and fracability not equivalent in designing hydraulic fracturing in tight shale gas reservoirs. *Petroleum, 2(1),* 1–19. DOI 10.1016/j.petlm.2016.01.001.

80. East, L., Soliman M, Y., Augustine, J. (2011). Methods for enhancing far-field complexity in fracturing operations. *SPE Production & Operations, 26(3),* 291–303. DOI 10.2118/133380-PA.

81. Guo, L., Fahs, M., Hoteit, H., Gao, R., Shao, Q. (2021). Uncertainty analysis of seepage-induced consolidation in a fractured porous medium. *Computer Modeling in Engineering & Sciences, 129(1),* 279–297. DOI 10.32604/cmes.2021.016619.

82. Zhang, H., Wan, Z., Zhao, Y., Zhang, Y., Chen, Y. et al. (2021). Shear induced seepage and heat transfer evolution in a single-fractured hot-dry-rock. *Computer Modeling in Engineering & Sciences, 126(2),* 442–454. DOI 10.32604/cmes.2021.013179.
83. Kundert, D. P., Mullen, M. J. (2009). Proper evaluation of shale gas reservoirs leads to a more effective hydraulic-fracture stimulation. *SPE Rocky Mountain Petroleum Technology Conference*, Denver, Colorado. DOI 10.2118/123586-ms.
84. Johri, M., Zoback, M. D. (2013). The evolution of stimulated reservoir volume during hydraulic stimulation of shale Gas formations. *Unconventional Resources Technology Conference*, pp. 12–14. Denver, Colorado. DOI 10.1190/urtec2013-170.
85. Hou, B., Zhang, R., Zeng, Y., Fu, W., Muhadasi, Y. et al. (2018). Analysis of hydraulic fracture initiation and propagation in deep shale formation with high horizontal stress difference. *Journal of Petroleum Science and Engineering, 170,* 231–243. DOI 10.1016/j.petrol.2018.06.060.
86. Tan, P., Pang, H., Zhang, R., Jin, Y., Zhou, Y. et al. (2020). Experimental investigation into hydraulic fracture geometry and proppant migration characteristics for southeastern sichuan deep shale reservoirs. *Journal of Petroleum Science and Engineering, 184,* 106517. DOI 10.1016/j.petrol.2019.106517.
87. Ren, L., Lin, R., Zhao, J., Rasouli, V., Zhao, J. et al. (2018). Stimulated reservoir volume estimation for shale gas fracturing, mechanism and modeling approach. *Journal of Petroleum Science and Engineering, 166,* 290–304. DOI 10.1016/j.petrol.2018.03.041.
88. Samuelson, M., Stefanski, J., Downie, R., Mikhaylov, A., Ovsyannikov, D. et al. (2012). Field development study, channel fracturing achieves both operational and productivity goals in the barnett shale. *SPE Americas Unconventional Resources Conference*, Pittsburgh, Pennsylvania USA. DOI 10.2118/155684-MS.
89. Gomes R, C. (2013). Effect of stress disturbance induced by construction on the seismic response of shallow bored tunnels. *Computers and Geotechnics, 49,* 338–351. DOI 10.1016/j.compgeo.2012.09.007.
90. Edelsbrunner, H., Valtr, P., Welzl, E. (1997). Cutting dense point sets in half. *Discrete & Computational Geometry, 17(3),* 243–255. DOI 10.1007/PL00009291.
91. Yin, J., Guo, J. C., Zeng, F. H. (2012). Perforation spacing optimization for staged fracturing of horizontal well. *Petroleum Drilling Techniques, 40(5),* 67–71. DOI 10.3969/J.ISSN.1001-0809.2012.05.015.
92. Wanniarachchi, W. A. M., Ranjith, P. G., Perera, M. S. A. (2017). Shale gas fracturing using foam-based fracturing fluid: A review. *Environmental Earth Sciences, 76(2),* 1–15. DOI 10.1007/s12665-017-6399-x.
93. Shaefer, M. T. (2005). Are slick water-fracturing applications effective in the J-sand formation? *SPE Annual Technical Conference and Exhibition*, Dallas, Texas, USA. DOI 10.2118/96933-ms.
94. Woodworth, T. R., Miskimins, J. L. (2007). Extrapolation of laboratory proppant placement behavior to the field in slickwater fracturing applications. *SPE Hydraulic Fracturing Technology Conference*, College Station, Texas, USA. DOI 10.2118/106089-ms.
95. Palisch, T. T., Vincent, M. C., Handren, P. J. (2010). Slickwater fracturing, food for thought. *SPE Production & Operations, 25(3),* 327–344. DOI 10.2118/115766-PA.
96. Pang, H., Meng, H., Wang, H., Fan, Y., Nie, Z. et al. (2022). Lost circulation prediction based on machine learning. *Journal of Petroleum Science and Engineering, 208,* 109364. DOI 10.1016/j.petrol.2021.109364.
97. Yang, C., Feng, W., Zhou, F. (2020). Formation of temporary plugging in acid-etched fracture with degradable diverters. *Journal of Petroleum Science and Engineering, 194,* 107535. DOI 10.1016/j.petrol.2020.107535.
98. Deng, S., Li, H., Ma, G., Huang, H., Li, X. (2014). Simulation of shale–proppant interaction in hydraulic fracturing by the discrete element method. *International Journal of Rock Mechanics and Mining Sciences, 70,* 219–228. DOI 10.1016/j.ijrmms.2014.04.011.
99. Alramahi, B., Sundberg, M. I. (2012). Proppant embedment and conductivity of hydraulic fractures in shales. *46th US Rock Mechanics/Geomechanics Symposium*, Chicago, Illinois.

100. Elgmati, M. M., Zhang, H., Bai, B., Flori, R. E., Qu, Q. (2011). Submicron-pore characteri-zation of shale gas plays. *North American Unconventional Gas Conference and Exhibition*, The Woodlands, Texas, USA. DOI 10.2118/144050-ms.

101. White C, M., Mungal M, G. (2008). Mechanics and prediction of turbulent drag reduction with polymer additives. *Annual Review of Fluid Mechanics, 40,* 235–256. DOI 10.1146/annurev.fluid.40.111406.102156.

102. Roussel, N. P., Sharma, M. M. (2011). Strategies to minimize frac spacing and stimulate natural fractures in horizontal completions. *SPE Annual Technical Conference and Exhibition,* Denver, Colorado, USA. DOI 10.2118/146104-ms.

103. Liu, R., Jiang, Y., Huang, N., Sugimoto, S. (2018). Hydraulic properties of 3D crossed rock fractures by considering anisotropic aperture distributions. *Advances in Geo-Energy Research, 2(2),* 113–121. DOI 10.26804/ager.

104. Tan, P., Jin, Y., Pang, H. (2021). Hydraulic fracture vertical propagation behavior in transversely isotropic layered shale formation with transition zone using XFEM-based CZM method. *Engineering Fracture Mechanics, 248,* 107707. DOI 10.1016/j.engfracmech.2021.107707.

105. Pang, H., Jin, Y., Gao, Y. (2019). Evaluation of elastic property changes in karamay oil sand reservoir during thermal stimulation. *Energy Science & Engineering, 7(4),* 1233–1253. DOI 10.1002/ese3.342.

106. Daneshy, A., King, G. (2019). Horizontal well frac-driven interactions, types, consequences, and damage mitigation. *Journal of Petroleum Technology, 71(6),* 45–47. DOI 10.2118/0619-0045-JPT.

107. Wu, R., Kresse, O., Weng, X., Cohen, C. -E., Gu, H. (2012). Modeling of interaction of hydraulic fractures in complex fracture networks. *SPE Hydraulic Fracturing Technology Conference*, The Woodlands, Texas, USA. DOI 10.2118/152052-ms.

108. Wu, K., Olson, J. E. (2015). Simultaneous multifracture treatments, fully coupled fluid flow and fracture mechanics for horizontal wells. *SPE Journal, 20(2),* 337–346. DOI 10.2118/167626-PA.

109. Wu, K., Olson, J., Balhoff, M. T., Yu, W. (2017). Numerical analysis for promoting uniform development of simultaneous multiple-fracture propagation in horizontal wells. *SPE Production & Operations, 32(1),* 41–50. DOI 10.2118/174869-PA.

110. Guo, X., Wu, K., Killough, J. (2018). Investigation of production-induced stress changes for infill-well stimulation in eagle ford shale. *SPE Journal, 23(4),* 1372–1388. DOI 10.2118/189974-PA.

111. Han, Y. L., Liu, Z. B., Cheng, Z. Y., Peng, Z. H. A. N. G. Hongyun, Zhang, P., Zhan, H. Y. (2011). The development and application of the sectional fracture sliding sleeve in horizontal wells. *China Petroleum Machinery, 39(2),* 64–65. DOI 10.16082/j.cnki.issn.1001-4578.2011.02.020.

112. Yunlong, D., Shizhong, T., Yanhua, N., Zhaopeng, L. V., Xiaobin, W. (2013). Problems and measurements of sliding sleeve staged fracturing completionin casing cementing horizontal wells. *Oil Drilling & Production Technology, 35(1),* 28–30. DOI 10.13639/j.odpt.2013.01.008.

113. Yang, H., Wang, R., Zhou, W., Li, L., Chen, F. (2014). A study of influencing factors on fracture initiation pressure of cemented sliding sleeve fracturing. *Journal of Natural Gas Science and Engineering, 18,* 219–226. DOI 10.1016/j.jngse.2014.03.002.

114. Cipolla, C. L., Mack, M. G., Maxwell, S. C. (2010). Reducing exploration and appraisal risk in Low-permeability reservoirs using microseismic fracture mapping. *Canadian Unconventional Resources and International Petroleum Conference*, Calgary, Alberta, Canada. DOI 10.2118/137437-ms.

115. Cipolla, C. L., Mack, M. G., Maxwell, S. C. (2010). Reducing exploration and appraisal risk in Low permeability reservoirs using microseismic fracture mapping–Part 2. *SPE Latin American and Caribbean Petroleum Engineering Conference*, Lima, Peru. DOI 10.2118/138103-ms.

116. Warpinski, N. R., Mayerhofer, M. J., Vincent, M. C., Cipolla, C. L., Lolon, E. P. (2009). Stimulating unconventional reservoirs, maximizing network growth while optimizing fracture conductivity. *Journal of Canadian Petroleum Technology, 48(10),* 39–51. DOI 10.2118/114173-PA.

117. Das, I., Zoback, M. D. (2011). Long-period, long-duration seismic events during hydraulic fracture stimulation of a shale gas reservoir. *The Leading Edge, 30(7),* 778–786. DOI 10.1190/1.3609093.

118. Liu, X., Jin, Y., Lin, B. (2021). An efficient stimulated reservoir area (SRA) estimation method based on octree decomposition of microseismic events. *Journal of Petroleum Science and Engineering, 198,* 108291. DOI 10.1016/j.petrol.2020.108291.
119. Liu, X., Jin, Y., Lin, B., Zhang, Q., Wei, S. (2021b). An integrated 3D fracture network reconstruction method based on microseismic events. *Journal of Natural Gas Science and Engineering, 95,* 104182. DOI 10.1016/j.jngse.2021.104182.
120. Zhang, Q., Hou, B., Lin, B., Liu, X., Gao, Y. (2021). Integration of discrete fracture reconstruction and dual porosity/dual permeability models for gas production analysis in a deformable fractured shale reservoir. *Journal of Natural Gas Science and Engineering,* 104028. DOI 10.1016/j.jngse.2021.104028.
121. Ellmauthaler, A., Palacios, W., LeBlanc, M., Willis, M., Knapo, G. (2019). Vertical seismic profiling via coiled tubing-conveyed distributed acoustic sensing. *SPE/ICoTA Well Intervention Conference and Exhibition*, The Woodlands, Texas, USA. DOI 10.2118/194244-ms.
122. Cui, J., Yang, C., Zhu, D., Datta-Gupta, A. (2016). Fracture diagnosis in multiple-stage-stimulated horizontal well by temperature measurements with fast marching method. *SPE Journal, 21(6),* 2289–2300. DOI 10.2118/174880-PA.
123. Stokely C, L. (2016). Acoustics-based flow monitoring during hydraulic fracturing. *SPE Hydraulic Fracturing Technology Conference*, The Woodlands, Texas, USA. DOI 10.2118/179151-ms.
124. Sun, H., Yu, W., Sepehrnoori, K. (2017). A new comprehensive numerical model for fracture diagnosis with distributed temperature sensing DTS. *SPE Annual Technical Conference and Exhibition*, San Antonio, Texas, USA. DOI 10.2118/187097-ms.
125. Holley, E. H., Molenaar, M. M., Fidan, E., Banack, B. (2013). Interpreting uncemented multistage hydraulic-fracturing completion effectiveness by use of fiber-optic DTS injection data. *SPE Drilling & Completion, 28(3),* 243–253. DOI 10.2118/153131-PA.
126. Nath, D. K., Finley, D. B., Kaura, J. D. (2006). Real-time fiber-optic distributed temperature sensing (DTS)-New applications in the oilfield. *SPE Annual Technical Conference and Exhibition*. DOI 10.2118/103069-ms.
127. Settgast, R. R., Fu, P., Walsh, S. D., White, J. A., Annavarapu, C. et al. (2017). A fully coupled method for massively parallel simulation of hydraulically driven fractures in 3-Dimensions. *International Journal for Numerical and Analytical Methods in Geomechanics, 41(5),* 627–653. DOI 10.1002/nag.2557.
128. Cao, R., Li, R., Chen, C., Girardi, A. (2017). Well interference and optimum well spacing for wolfcamp development at Permian Basin. *Proceedings of the 5th Unconventional Resources Technology Conference*. DOI 10.15530/urtec-2017-2691962.
129. Willberg, D. M., Steinsberger, N., Hoover, R., Card, R. J., Queen, J. (1998). Optimization of fracture cleanup using flowback analysis. *SPE Rocky Mountain Regional/Low-Permeability Reservoirs Symposium*. DOI 10.2118/39920-ms.
130. Simpson, J. P., Walker, T. O., Jiang, G. Z. (1995). Environmentally acceptable water-base mud can prevent shale hydration and maintain borehole stability. *SPE Drilling & Completion, 10(4),* 242–249. DOI 10.2118/27496-PA.
131. Tianshou M, A., Ping, C. (2014). Study of meso-damage characteristics of shale hydration based on CT scanning technology. *Petroleum Exploration and Development, 41(2),* 249–256. DOI 10.1016/S1876-3804(14)60029-X.
132. Du, W., Wang, X., Chen, G., Zhang, J., Slaný, M. (2020). Synthesis, property and mechanism analysis of a novel polyhydroxy organic amine shale hydration inhibitor. *Minerals, 10(2),* 128. DOI 10.3390/min10020128.
133. Shen, W., Li, X., Cihan, A., Lu, X., Liu, X. (2019). Experimental and numerical simulation of water adsorption and diffusion in shale gas reservoir rocks. *Advances in Geo-Energy Research, 3(2),* 165–174. DOI 10.26804/ager.

134. Dehghanpour, H., Zubair, H. A., Chhabra, A., Ullah, A. (2012). Liquid intake of organic shales. *Energy & Fuels, 26(9),* 5750–5758. DOI 10.1021/ef3009794.

135. Dehghanpour, H., Lan, Q., Saeed, Y., Fei, H., Qi, Z. (2013). Spontaneous imbibition of brine and oil in gas shales, effect of water adsorption and resulting microfractures. *Energy & Fuels, 27(6),* 3039–3049. DOI 10.1021/ef4002814.

136. Pagels, M., Hinkel, J. J., Willberg, D. M. (2012). Measuring capillary pressure tells more than pretty pictures. *SPE International Symposium and Exhibition on Formation Damage Control*, San Antonio, Texas, USA. DOI 10.2118/151729-ms.

137. Bennion, D. B., Thomas, F. B., Bietz, R. F., Bennion, D. W. (1996). Water and hydrocarbon phase trapping in porous media-diagnosis, prevention and treatment. *Journal of Canadian Petroleum Technology, 35(10),* DOI 10.2118/96-10-02.

138. Wang, F., Pan, Z. Q. (2016). Numerical simulation of chemical potential dominated fracturing fluid flowback in hydraulically fractured shale gas reservoirs. *Petroleum Exploration and Development, 43(6),* 1060–1066. DOI 10.1016/S1876-3804(16)30123-9.

139. Penny, G., Dobkins, T., Pursley, J. (2006). Field study of completion fluids to enhance Gas production in the barnett shale. *Proceedings of SPE gas Technology Symposium*, Calgary, Alberta, Canada. DOI 10.2523/100434-ms.

140. Robinson, B. M., Holditch, S. A., Whitehead, W. S. (1988). Minimizing damage to a propped fracture by controlled flowback procedures. *Journal of Petroleum Technology, 40(6),* 753–759. DOI 10.2118/15250-PA.

141. Huang, J., Hu, J., Zeng, W., Zhang, Y. (2019). Investigation of a critical choke during hydraulic-fracture flowback for a tight sandstone gas reservoir. *Journal of Geophysics and Engineering, 16(6),* 1178–1190. DOI 10.1093/jge/gxz088.

142. Jacobs, T. (2015). Improving shale production through flowback analysis. *Journal of Petroleum Technology, 67(12),* 37–42. DOI 10.2118/1215-0037-JPT.

143. Lin, B., Guo, J., Liu, X., Xiang, J., Zhong, H. (2020). Prediction of flowback ratio and production in sichuan shale gas reservoirs and their relationships with stimulated reservoir volume. *Journal of Petroleum Science and Engineering, 184,* 106529. DOI 10.1016/j.petrol.2019.106529.

144. Chen, Y., Ma, G., Wang, H. (2018). Heat extraction mechanism in a geothermal reservoir with rough-walled fracture networks. *International Journal of Heat and Mass Transfer, 126,* 1083–1093. DOI 10.1016/j.ijheatmasstransfer.2018.05.103.

145. Chen, Y., Ma, G., Wang, H., Li, T. (2018). Evaluation of geothermal development in fractured hot dry rock based on three dimensional unified pipe-network method. *Applied Thermal Engineering, 136,* 219–228. DOI 10.1016/j.applthermaleng.2018.03.008.

146. Ma, G., Chen, Y., Jin, Y., Wang, H. (2018). Modelling temperature-influenced acidizing process in fractured carbonate rocks. *International Journal of Rock Mechanics and Mining Sciences, 105,* 73–84. DOI 10.1016/j.ijrmms.2018.03.019.